

Kerogen characterization of the Vaca Muerta Formation (Tithonian-Valanginian), at Mallín Quemado and Puerta Curaco, Neuguén Basin, central-west Patagonia, Argentina. Palynofacies and geochemical approach

LUIS SEBASTIÁN AGÜERO<sup>1,2</sup> DANIELA ELIZABETH OLIVERA<sup>3</sup> MARCELO ADRIÁN MARTÍNEZ<sup>1,2</sup> GERMÁN OTHARÁN

- 1. Instituto Geológico del Sur (INGEOSUR). Universidad Nacional del Sur (UNS) Consejo Nacional de Investigaciones Científicas y Técnicas (CONICET). Avenida Alem 1253, B8000ICN Bahía Blanca, Buenos Aires, Argentina.
- 2. Departamento de Geología, Universidad Nacional del Sur (UNS) Consejo Nacional de Investigaciones Científicas y Técnicas (CONICET). Avenida Alem 1253, B8000ICN Bahía Blanca, Buenos Aires, Argentina.
- 3. Shandong Provincial Key Laboratory of Depositional Mineralization and Sedimentary Minerals, Shandong University of Science and Technology. Qianwangang Road 579, 266590 Qingdao, Shandong Province, China.
- 4. Yacimientos Petrolíferos Fiscales (YPF). Talero 360, Q8300IEH Neuquén, Neuquén, Argentina

Recibido: 1 de julio de 2025 - Aceptado: 9 de septiembre de 2025 - Publicado: 3 de noviembre de 2025

Para citar este artículo: Luis Sebastián Agüero, Daniela Elizabeth Olivera, Marcelo Adrián Martínez, & Germán Otharán (2025). Kerogen characterization of the Vaca Muerta Formation (Tithonian-Valanginian), at Mallín Quemado and Puerta Curaco, Neuquén Basin, central-west Patagonia, Argentina. Palynofacies and geochemical approach. Publicación Electrónica de la Asociación Paleontológica Argentina 25(2): 155-182.

Link a este artículo: http://dx.doi.org/10.5710/PEAPA.09.09.2025.548

©2025 Agüero, Olivera, Martínez, Otharán



Asociación Paleontológica Argentina Maipú 645 1º piso, C1006ACG, Buenos Aires

República Argentina Tel/Fax (54-11) 4326-7563

Web: www.apaleontologica.org.ar











# KEROGEN CHARACTERIZATION OF THE VACA MUERTA FORMATION (TITHONIAN-VALANGINIAN), AT MALLÍN QUEMADO AND PUERTA CURACO, NEUQUÉN BASIN, CENTRAL-WEST PATAGONIA, ARGENTINA. PALYNOFACIES AND GEOCHEMICAL **APPROACH**

LUIS SEBASTIÁN AGÜERO<sup>1,2</sup>, DANIELA ELIZABETH OLIVERA<sup>3</sup>, MARCELO ADRIÁN MARTÍNEZ<sup>1,2</sup>, AND GERMÁN OTHARÁN<sup>4</sup>

Instituto Geológico del Sur (INGEOSUR), Universidad Nacional del Sur (UNS) – Consejo Nacional de Investigaciones Científicas y Técnicas (CONICET), Avenida Alem 1253, B8000ICN Bahía Blanca, Buenos Aires, Argentina. luisaguero@ingeosur-conicet.gob.ar, martinez@criba.edu.ar

<sup>2</sup>Departamento de Geología, Universidad Nacional del Sur (UNS) – Consejo Nacional de Investigaciones Científicas y Técnicas (CONICET). Avenida Alem 1253, B8000ICN Bahía Blanca, Buenos Aires, Argentina.

<sup>3</sup>Shandong Provincial Key Laboratory of Depositional Mineralization and Sedimentary Minerals, Shandong University of Science and Technology. Qianwangang Road 579, 266590 Qingdao, Shandong Province, China. daniela.olivera@uns.edu.ar

"Yacimientos Petrolíferos Fiscales (YPF). Talero 360, Q8300IEH Neuquén, Neuquén, Argentina. german.otharan@ypf.com



6 LSA: https://orcid.org/0009-0003-5590-5544; DEO: https://orcid.org/0000-0001-9291-9935; MAM: https://orcid.org/0000-0003-0538-4739; GO: https://orcid.org/0000-0002-5872-1105

Abstract. This contribution integrates palynofacies, organic geochemical and sedimentological analyses to characterize the depositional environment and the kerogen properties related to the hydrocarbon source potential of the Vaca Muerta Formation at the Mallín Quemado Norte (MQN) and Puerta Curaco (PC), Neuquén Basin, Argentina. Thirty-five outcrop samples were analyzed for palynofacies and total organic carbon (TOC). At MQN, five palynofacies types and sedimentological evidence suggest deposition mainly in an outer shelf marine environment with a variable continental input. At PC, three palynofacies types and sedimentological observations point to accumulation mainly in an outer ramp marine environment with minimal to moderate terrigenous input. Depositional processes involve an interplay of suspension settling from the water column (marine snow) and buoyant plumes, followed by reworking of the seafloor by bottom currents and sediment gravity flows. Under identical hydrodynamic flow conditions, equidimensional phytoclasts respond better to transport sorting than blade-shaped. The first documentation of high-relief organic spheres (HROS) in this unit points to redox oscillation between sulfidic and ferruginous anoxic microenvironments during early diagenesis. Low HROS percentages and crypto-bioturbated strata suggest that bottom waters were not strictly anoxic. Organic carbon preservation may be partly related to the role of extracellular polymeric substances as an organic matter encapsulator. The kerogen aligns with type III-IV, and TOC values are mainly high (MQN: up to 4.69%; PC: 4.9-10.4%). Although an over-mature state cannot be entirely ruled out (highly dark palynological matter), the poor preservation of the kerogen suggests a negligible hydrocarbon potential.

Key words. Vaca Muerta Formation. Kerogen. Palynofacies analysis. Total organic carbon. Paleoenvironment. Hydrocarbon source potential.

Resumen. CARACTERIZACIÓN DEL QUERÓGENO DE LA FORMACIÓN VACA MUERTA (TITONIANO-VALANGINIANO), EN MALLÍN QUEMADO Y PUERTA CURACO, CUENCA NEUQUINA, CENTRO-OESTE DE LA PATAGONIA, ARGENTINA. ENFOQUE PALINOFACIAL Y GEOQUÍMICO. Esta contribución integra análisis palinofacial, geoquímico orgánico y sedimentológico para caracterizar el ambiente depositacional y las propiedades del querógeno asociadas al potencial de roca madre de hidrocarburos de la Formación Vaca Muerta en Mallín Quemado Norte (MQN) y Puerta Curaco (PC), Cuenca Neuquina, Argentina. Se analizaron 35 muestras para palinofacies y carbono orgánico total (COT). En MQN, cinco palinofacies tipo y evidencia sedimentológica sugieren depositación principalmente en ambiente marino de plataforma externa con aporte continental variable. En PC, tres palinofacies tipo y observaciones sedimentológicas sugieren acumulación principalmente en ambiente marino de rampa externa con aporte terrígeno mínimo a moderado. Los procesos depositacionales involucran interacción entre decantación desde columna de agua (nieve marina) y plumas flotantes, con retrabajo posterior del fondo marino por corrientes y flujos gravitacionales. Bajo condiciones hidrodinámicas idénticas, los fitoclastos equidimensionales responden mejor a la selección por transporte que los con forma de tablilla. El primer registro de esferas orgánicas de alto relieve (HROS) en esta unidad apunta a oscilación redox entre microambientes anóxicos sulfídicos y ferruginosos durante la diagénesis temprana. Bajos porcentajes de HROS y estratos criptobioturbados sugieren aguas del fondo no estrictamente anóxicas. La preservación del carbono orgánico podría estar parcialmente relacionada con sustancias poliméricas extracelulares encapsuladoras de materia orgánica. El querógeno se alinea con el tipo III-IV y los valores de COT son principalmente altos (MQN: hasta 4.69%; PC: 4.9-10.4%). Aunque no puede descartarse totalmente un estado de sobremadurez (materia palinológica altamente oscura), la pobre preservación del querógeno sugiere un potencial de hidrocarburos negligible.

Palabras clave. Formación Vaca Muerta. Querógeno. Análisis palinofacial. Carbono orgánico total. Paleoambiente. Potencial como fuente de hidrocarburos.



THE UPPER Jurassic—Lower Cretaceous Vaca Muerta Formation (Weaver, 1931) is the main source rock of the Neuquén Basin (Legarreta & Villar, 2011; Stinco & Barredo, 2014). It hosts the largest unconventional hydrocarbon resources in Argentina and the third largest in the world (Minisini *et al.*, 2020a). Since 2010, different companies started drilling exploration wells targeting the unconventional oil and gas shales from the Vaca Muerta Formation.

In recent years, knowledge of the Vaca Muerta Formation has increased significantly from different approaches: paleontological (*e.g.*, Aguirre-Urreta *et al.*, 2019; Kietzmann *et al.*, 2022), micropaleontological (*e.g.*, Agüero *et al.*, 2022; Olivera *et al.*, 2023), sedimentological (*e.g.*, Otharán *et al.*, 2018, 2022; Paz *et al.*, 2022), tectono-stratigraphic (*e.g.*, Ramos *et al.*, 2019; Domínguez *et al.*, 2020) and oleogenetic potential (*e.g.*, Brisson *et al.*, 2020; Minisini *et al.*, 2020b), among others. Additionally, studies of the geological properties of the Vaca Muerta Formation have been the subject of books (*e.g.*, González *et al.*, 2016; Minisini *et al.*, 2020a). Nevertheless, palynofacies analysis of the Vaca Muerta Formation remain scarce, with only a few contributions focused on the analysis of the palynology of this unit (Otharán *et al.*, 2022).

The main objectives of this research are: i) to characterize the kerogen of the Vaca Muerta Formation in outcrop samples collected at Mallín Quemado Norte and Puerta Curaco localities, and ii) to evaluate the depositional environment and the hydrocarbon source potential of these levels. This contribution is approached from a multidisciplinary perspective, which includes palynological organic matter (palynofacies), sedimentological and organic geochemical analysis.

#### **GEOLOGICAL BACKGROUND**

The Neuquén Basin is located in central western Argentina between 32°-40°S (Fig. 1). It has a subtriangular shape that covers an area of approximately 120,000 km² (Yrigoyen, 1991). It is limited to the west by the Andean magmatic arc, to the northeast by the Sierra Pintada System and to the southeast by the Nordpatagonian Massif. The basin has a Meso-Cenozoic sedimentary infill of approximately 7000 m, including siliciclastic continental and marine sediments, carbonates, evaporites, volcanic and volcaniclastic deposits

(Howell et al., 2005; Arregui et al., 2011).

Internally, this succession can be subdivided into three major sedimentary cycles: "Jurásico", "Ándico" and " Riográndico" (Groeber, 1946), which are separated by regional unconformities. The Ándico Cycle comprises the Mendoza (Stipanicic et al., 1968) and the Bajada del Agrio groups (Méndez et al., 1995). The Mendoza Group is composed by three Mesosequences, named Lower, Middle and Upper (Legarreta & Gulisano, 1989). The Lower Mesosequence (early Kimmeridgian-early Valanginian) starts with continental deposits (i.e., lacustrine, alluvial fan, fluvial and aeolian) (Zavala et al., 2008; Leanza, 2009) of the Tordillo Formation (Groeber, 1946). This Mesosequence finishes with the Vaca Muerta Formation which overlies the Tordillo Formation in sharp contact. The Vaca Muerta Formation is mainly composed of organic carbon-rich mudstones (average 3.2 per cent by weight TOC, maximum ~15% TOC; Brisson et al., 2020) with thin volcaniclastic layers, limestone and minor sandstone deposits (Leanza et al., 2003; Kietzmann et al., 2014; Minisini et al., 2020b; Naipauer et al., 2020; Otharán, 2020). It was accumulated during the early Tithonian-early Valanginian (Groeber, 1946; Leanza, 1973; Leanza & Hugo, 1977; Aguirre-Urreta et al., 2019) throughout the Neuquén Basin, reaching a maximum thickness of 1400 m at the locality of Arroyo Mulichinco and a minimum of 129 m near Cerro Lotena (Leanza, 1973; Otharán et al., 2020).

The studied outcrops of the Vaca Muerta Formation are located at Mallín Quemado Norte (MQN, 45 km NW of Zapala city) and Puerta Curaco (PC, 30 km E of Chos Malal city), both located in the central depositional sites of the Neuquén Basin (Fig. 1). In MQN, this unit reaches a thickness of 842.5 m and is mainly composed of organic carbon-rich and calcareous mudstones interbedded with limestones, concretionary horizons and thin-bedded ash layers, with minor participation of fine grained, lenticular sandstone beds (Fig. 2.1). In PC, the Vaca Muerta Formation is 541.7 m thick and comprises a succession of organic carbon-rich mudstones and calcareous mudstones interbedded with limestones as well as concretionary beds and ash beds (Fig. 2.2).

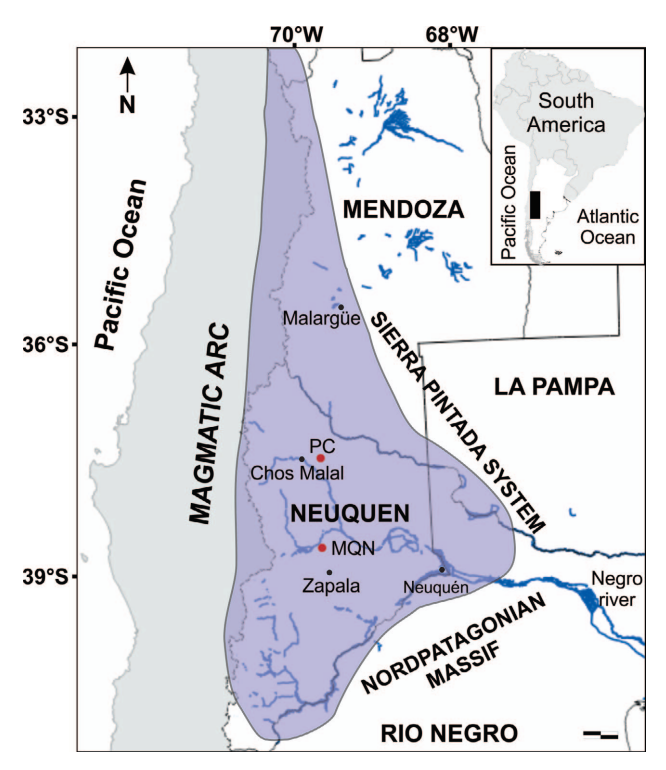


**Figure 1.** The Neuquén Basin, central western Argentina, with indication of studied localities. Abbreviations: **MQN**, Mallín Quemado Norte; **PC**, Puerta Curaco. Scale bar= 50 km.

# **MATERIALS AND METHODS**

# Sampling, laboratory and microscopy techniques

A total of thirty-five outcrop samples from the Vaca Muerta Formation at Mallín Quemado Norte (19) and Puerta Curaco (16) localities were processed for palynological and total organic carbon analyses (Fig. 2). The preparation of palynological samples was carried out using standard techniques, including treatment with hydrochloric and hydrofluoric acids (Volkheimer & Melendi, 1976). No oxidation by nitric acid was performed because it affects the color and preservation of the organic particles (Volkheimer & Melendi, 1976).

The slides were analyzed using transmitted white light (TWL) microscope (Olympus BH-2). Additionally, the palynological matter (PM) constituents were evaluated using reflected fluorescence light (RFL) microscope (Olympus BH-2) to interpret their preservation state and to determine the hydrocarbon-source potential (Tyson, 1995).

The palynological slides are housed at the Instituto Geológico del Sur-Universidad Nacional del Sur, Bahía Blanca, Buenos Aires Province, Argentina. The specimens are identified with the slide number and corresponding England Finder coordinates (EF).

## Statistical analysis

The distribution of palynomorphs is based on the count of 250 specimens per sample. Palynomorphs were classified into six main groups subdivided according to their biological affinities: spores, pollen grains (Hirmeriellaceae, Araucariaceae, Pinaceae, Podocarpaceae, Caytoniaceae, Cycadales/Ginkgoales/Bennettitales and Ephedraceae), organic-walled fresh-water microplankton (OWFWM), organic-walled marine microplankton (OWMM, prasinophytes, acritarchs and dinocysts), fungal spores and bacteria remains (coccoids). The statistical count excludes coccoids because of their high abundance in some amorphous masses. Palynomorphs relative frequencies (%) distribution were plotted in pie charts.

To quantify the palynofacies components, 500 particles of PM larger than 10 µm were counted per sample/ preparation using a 40x magnification following Tyson (1995). The PM was classified into structured organic matter (palynomorphs, non-discrete bacterial remains and phytoclasts) and structureless organic matter (AOM) following the categories proposed by Tyson (1995), Batten (1996a) and Oboh-Ikuenobe and de Villiers (2003). New divisions of AOM were created and described to accommodate material that did not fit into these established categories (laminated, bAOMte, gAOMtm and transparent). Detailed descriptions of these categories are provided in Table 1. The relative frequencies (%) bar diagrams were calculated using TGview 2.0.41 (Grimm, 2004). Then, the different constituents of the PM were interpreted in terms of palynofacies parameters (Tab. 2).

The count data obtained were statistically processed using the multivariate statistical program PAST (Palaeontological Statistics) by Hammer *et al.* (2001). Cluster analysis (Q-mode) based on composition and abundance (number of elements) was employed in order to define groups of samples and to recognize different associations of the PM (named as palynofacies types). It was performed with Euclidean distance and the unweighted pair group method (UPGM). Cluster analysis provides the cophenetic correlation coefficient as a measure of the relationship between



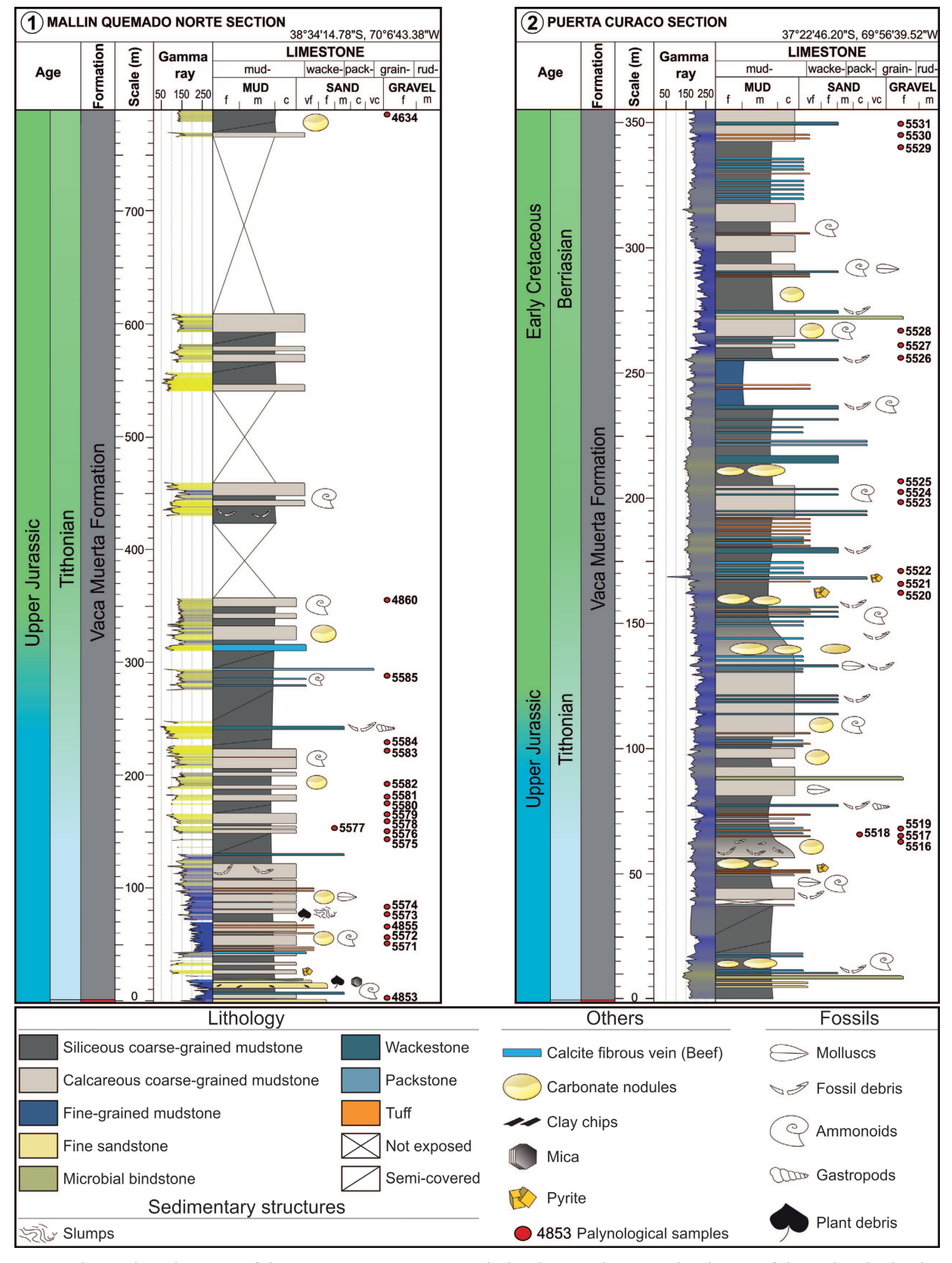


Figure 2. Sedimentological sections of the Vaca Muerta Formation studied in this contribution, with indication of the analyzed palynological samples. 1, Mallín Quemado Norte section. 2, Puerta Curaco section. Adapted from Olivera *et al.* (2018) and Otharán (2020).

| TABLE T - Clas | ssification of palyno               | iogicai organic mai                     | tter.                      |  |  |
|----------------|-------------------------------------|---|----------------------------|--|--|
| Group          | Categories                          |   |                            | Description  | Source   |
| Structured     | Palynomorphs                        | Sporomorphs                             | Spores and pollen grains   |  | Reproductive structures of vascular land plants  |
|                |                                     | Organic-walled<br>microplankton         | Fresh-water algae          |  | Chlorophyte algae  |
|                |                                     |   | Acritarchs                 |  | Organic-walled marine microplankton  |
|                |                                     |   | Prasinophytes              |  |  |
|                |                                     |   | Dinocysts                  |  |  |
|                |                                     | Fungal spores                           |                            |  | Reproductive structures of fungal origin   |
|                |                                     | Bacteria remains                        | Coccoids                   | Spherical elements of the order<br>of ca. 2–5 μm in diameter.<br>Commonly only recognizable<br>under RFL   | Fossil bacterial bodies  |
|                | Bacteria remains<br>(non-discrete)  | Filaments                               |                            | Elongated elements ca. 1 μm<br>wide and variable in length.<br>Translucent to light brown<br>under TWL and usually<br>folded/± coiled. Commonly only<br>recognizable under RFL | Bacteria derived   |
|                |                                     | Tubes                                   |                            | Structured or sometimes unstructured unbranched tubes  |  |
|                | Phytoclasts                         | Translucent                             | Tracheids with pits        |  | Macrophyte plant debris  |
|                |                                     |   | Tracheids without pits     |  |  |
|                |                                     |   | Other woody remains        |  |  |
|                |                                     |   | Cuticles                   |  |  |
|                |                                     |   | Membranes                  |  |  |
|                |                                     |   | Other tissue               |  |  |
|                |                                     |   | Dark brown-black fragments |  |  |
|                |                                     |   | Yellow-brown fragments     |  |  |
|                |                                     |   | Degraded fragments         | Dark brown-black fragments with corroded edges   |  |
|                |                                     |   | Gelified                   |  |  |
|                |                                     | Opaque                                  | Blade-shaped               |  |  |
|                |                                     |   | Equidimensional            |  |  |
| Structureless  | Amorphous orga-<br>nic matter (AOM) | Spongy                                  |                            |  | Mainly derived from degradation of continental algae   |
|                |                                     | Spongy-fibrous                          |                            |  | ?Continental origin  |
|                |                                     | Fibrous                                 |                            |  | Mainly derived from degradation of macrophyte tissues  |
|                |                                     | Membranous                              |                            |  | ,  |
|                |                                     | Granular                                |                            |  | Degradation of microplankton bacteria  |
|                |                                     | Pelicular <i>sensu</i><br>Combaz (1980) |                            |  | Degradation of microplankton<br>bacteria and/or to the second<br>product of microbial activity of<br>marine organic matter |
|                |                                     | Spongy-granular                         |                            |  | Microplankton derived  |
|                |                                     | Gelified                                |                            | Gelified brown AOM   | Terrestrially derived  |
|                |                                     | Resines                                 |                            |  | Natural secretions or exudations of higher plants  |



| ABLE 1 – Con  | ntinuation.                          |   |  |   |
|---------------|--------------------------------------|---|--|---|
| roup          | Categories                           |   | Description  | Source  |
| Structureless | Amorphous<br>organic matter<br>(AOM) | Laminated   | AOM ± laminated, brown, with ± lumpy internal appearance and irregular, crenulated and even almost straight edges. It shares some morphological similarities with bAOMte, so it is presumed that they are genetically related  | Mainly marine   |
|               |                                      | High-relief<br>organic<br>spheres <i>sensu</i><br>Emmings <i>et al.</i><br>(2019) | Orange-brownish spheres 8–18 µm in diameter with a ± rough to somewhat imperfectly reticulate wall. In optical cross-section the wall exhibits rounded or ± acuminate protrusions with rounded ends  | Sulfurized organic<br>matter local to pyrite<br>framboids |
|               |                                      | Pellets   | AOM of constant shape and size, subcylindrical and oval in outline   | Excrements of planktonic or benthic organisms             |
|               |                                      | bAOMte  | Dark brown to almost opaque<br>masses or laminae, ± elongated,<br>with irregular, straight, or often<br>somewhat diffuse, translucent<br>edges. May have crystals<br>imprints. Not fluorescent   | Mainly marine   |
|               |                                      | gAOMtm  | Transparent, to a lesser extent light to medium brown matrix with diffuse or sharp edges, which bind different particles. In some cases includes filamentous and coccoid bacteria. Fluoresce heterogeneously to yellow, green, orange, red, and all their combinations with weak, moderate or strong intensity. In the same sample they may fluoresce in different colors. Occasionally only recognizable by fluorescence. | Extracellular polymeric<br>substances (EPS)               |
|               |                                      | Transparent   | Masses that fluoresce moderately yellowish orange and containing short rod-shaped bacteria fluorescing moderately to strongly yellow. Not observable under transmitted light microscopy  | Extracellular polymeric substances (EPS)                  |

original distances and transformed final distances. According to Anderberg (1973) and Kovach (1989), this value should be close to 1 for high-quality resolution. Palynofacies types (PT) are defined on the quantitative total organic matter data and may reveal important information for paleoenvironmental interpretation (Brugman *et al.*, 1994 and references therein).

The majority of the phytoclasts identified in MQN belong to three categories: dark brown to black (DBBK), deteriorated (DET) and opaque (OP). In PC, most phytoclasts

correspond to the DBBK and OP categories. Since high percentages of these particles have been interpreted in a similar way (see Tyson, 1995), their proportions were added in each sample ("DBBK+DET+OP" for MQN, and "DBBK+OP" for PC) in order to recognize paleoenvironmental trends. Also, as phytoclasts behave like clastic particles (Traverse, 1994, among others), the "DBBK+DET+OP" (MQN) and "DBBK+OP" (PC) dimensions (in ranges) were evaluated to estimate the degree of deposits sorting. Additionally, we compared the size populations of equidimensional and

TABLE 2 – Summary of palynofacies parameters used for paleoenvironmental interpretation.

| Palynofacies parameters  | Palaeoenvironmental interpretation  | References                 |
|--|---|----------------------------|
| High % spores  | Proximity to active fluvio-deltaic source(s).   | 1, 3                       |
| High % phytoclasts of total PM                                       | Close proximity to, or redeposition from, fluvio-deltaic source(s) of terrestrial organic matter. (*) Especially applies in fluid flows; in the hyperpycnal flows the interpretation is opposite.  OR  Oxidizing environments in which other components have been selectively destroyed. TOC usually low, with high percentages of small opaque or semi-opaque phytoclasts. | 1, 2, 12                   |
| prasinophytes $\rightarrow$ acritarchs $\rightarrow$ dinoflagellates | Salinity gradient from restricted marginal marine (near shore) of reduced salinity to open-marine of normal salinity.   | 1, 4, 5, 6, 7,<br>8, 9, 10 |
| High % dinocysts (of total OWMM)                                     | Deposition beneath, or redeposition from, unstable, seasonal, shelf watermasses. Normal marine salinities.  | 1, 11                      |
| High % of ceratioids (of total dinocysts)                            | Shallow marine environment. Euryhaline conditions.  | 13, 14                     |

References: 1. Tyson (1995), 2. Batten (1996a), 3. Traverse (2007), 4. Martínez et al. (2008), 5. Martínez & Quattrocchio (2004), 6. Prauss (1989), 7. Prauss (1996), 8. Prauss (2001), 9. Prauss & Riegel (1989), 10. Brocke & Riegel (1996), 11. van de Schootbrugge et al. (2005), 12. Olivera et al. (2020), 13. Tahoun et al. (2018), 14. Garzon et al. (2012).

blade-shaped phytoclasts to evaluate their response to transport sorting.

In order to assess the terrigenous input along the sections in terms of periods of relative quiescence, low, moderate and high input, the following indicators were considered: (1) the paleoenvironmental information provided by each type of PM present in the PT, (2) the sorting of "DBBK+DET+OP" (MQN) and "DBBK+OP" (PC), (3) the changes in the trends of the total percentages of phytoclasts (allochthonous component) and the combined sum of granular AOM, spongy-granular AOM and pelicular AOM (autochthonous components) and (4) the sedimentary facies from which the PM was recovered.

# Hydrocarbon source potential analysis

To determine the potential of the studied levels as a source of hydrocarbons, the amount, type, thermal maturity and preservation state of the organic matter were evaluated.

The amount of organic matter was estimated by TOC analysis. In combination with palynofacies data, TOC measurements are a very useful parameter for assessing the depositional environment and source rock potential (Tyson, 1995; Batten, 1996b). To determine TOC, inorganic carbon was first removed from the samples. Following this, they were analyzed for TOC determination by dry

combustion using a LECO Automatic Carbon Analyzer, model CR-12. The results obtained are expressed as a percentage.

To assess whether the organic matter content in the studied deposits is sufficient for hydrocarbon generation, Cornford's quality scale (2005) was employed. This is a scale for shales and limestones based on the % of TOC. This scale classifies shales into six categories: very poor, poor, fair, good, very good and oil shale/carbargillite. A 'good' quality represents the threshold above which the organic matter content is considered sufficient for hydrocarbon generation.

The palynological kerogen type was evaluated following Tyson (1995), Batten (1996b) and Mendonça Filho *et al.* (2012). Type I kerogen corresponds to a highly oil-prone material; consists of strongly fluorescent organic matter comprising chlorococcal algae and prasinophytes and AOM derived from cyanobacteria and thiobacteria. Resins and cuticles are the only components of terrestrial origin that may be present in this kerogen. Type II kerogen corresponds to oil-prone material; fluorescent AOM is the main constituent, although fluorescent non-alginitic palynomorphs, as well as cuticular and membranous debris are also included. Type III kerogen corresponds to gas-prone material; includes biostructured translucent, generally brown and non-fluorescent phytoclasts, and non-biostructured translucent and non-fluorescent phytoclasts.



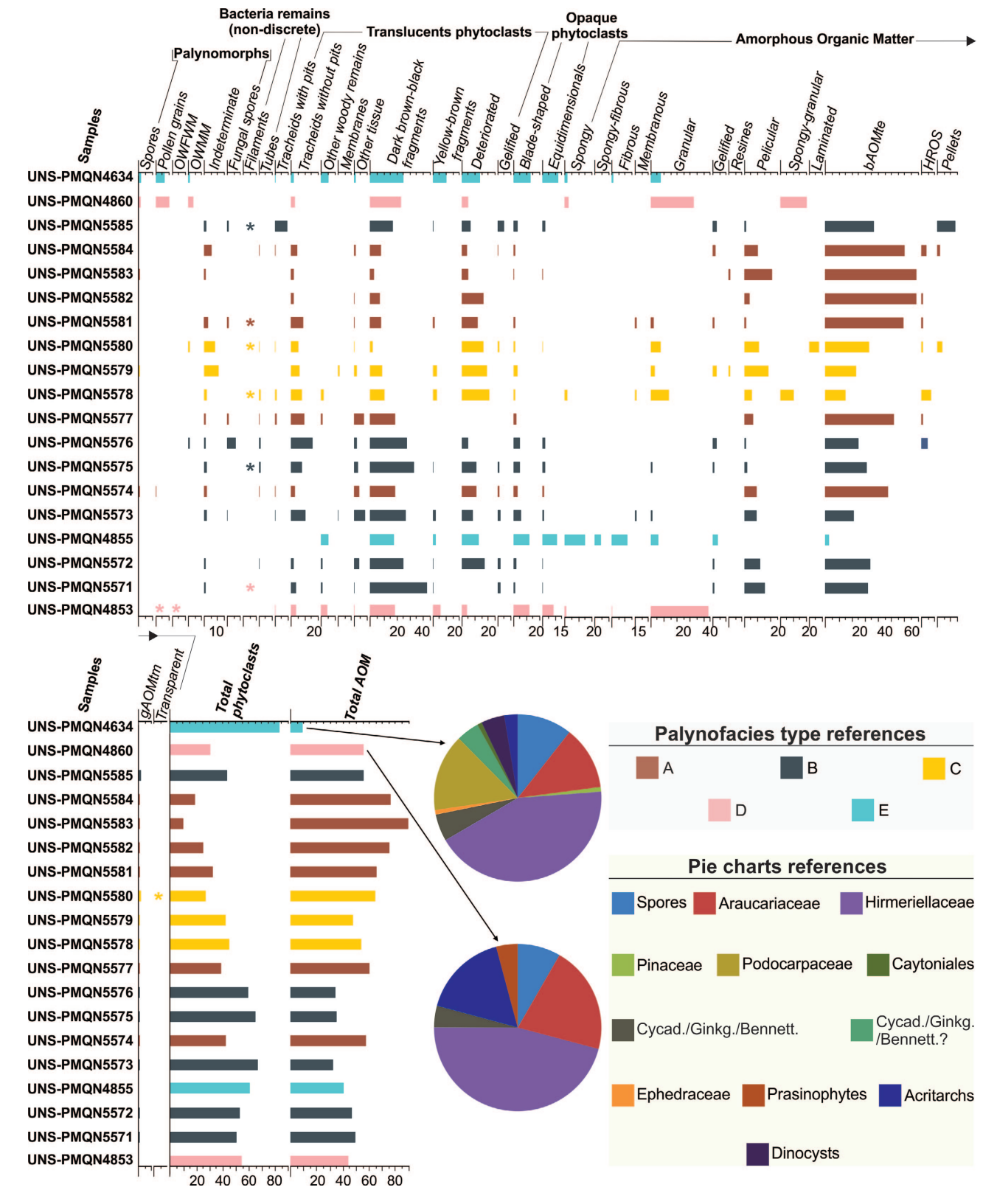


Figure 3. Relative frequency diagram (%) of the different palynological matter categories identified in the Mallín Quemado Norte section. Based on the total count of 500 particles per sample. \* indicates presence. The pie charts show the components of the palynomorph group identified in the two fertile samples.

Woody fragments, partially oxidized palynomorphs and plankton-derived material are typical. Type IV kerogen corresponds to inert material; it includes strongly oxidized, carbonized, opaque and non-fluorescent organic matter, such as opaque phytoclasts, fungal and chitinous material.

To estimate the thermal maturity of the organic matter, the color of the PM was qualitatively assessed (Salas & Seiler, 1980). This approach was used due to the poor preservation of psilate trilete spores and organic-walled microplankton, which precluded the use of the Thermal Alteration Index (TAI) scale of Staplin (1969).

The preservation state of the kerogen in all samples was evaluated by observing the characteristics of the PM, such as the preservation state of palynomorphs and the proportion of fragile and readily biodegradable tissue particles, using TWL and RFL (Tyson, 1995).

Abbreviations. AOM, structureless organic matter; DBBK, dark brown to black phytoclasts; DET, deteriorated phytoclasts; DS, depositional sequence; EF, England Finder coordinates; EQUID, equidimensional; EPS, extracellular polymeric substances; FRAM, framboid; HROS, high-relief organic spheres; MFS, maximum flooding surface; MQN, Mallín Quemado Norte; OP, opaque phytoclasts; OWFWM, organic-walled fresh-water microplankton; OWMM, organic-walled marine microplankton; PC, Puerta Curaco; PM, palynological matter; PT, palynofacies type; PY, pyrite; RFL, reflected fluorescence light; SB, sequence boundary; TAI, Thermal Alteration Index; TEP, transparent exopolymer particles; TOC, total organic carbon; TP, translucent particles; TS, transgressive surface; TWL, transmitted white light; UPGM, unweighted pair group method; W/N, within.

# **RESULTS**

# Mallín Quemado Norte section

Considering the relative variations of 34 PM types in the MQN section, five PT denominated A, B, C, D and E were identified from cluster analysis (Figs. 2–4). In all PT, most of the palynomorphs are poorly preserved. A selection of PM is illustrated on Figures 5.1–9 and 6.1–12.

PT A. This PT presents the highest percentage of the AOM group of all studied samples (56.8–89.6%), and within this, the highest values of black AOM with translucent edges (bAOMte) (47–69%). Four of the six samples contain high-

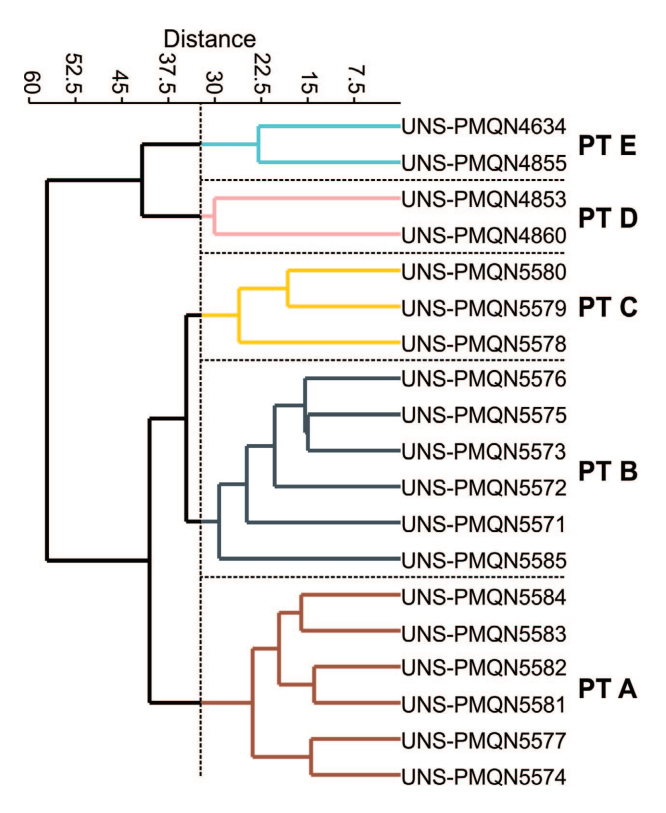


**Figure 4.** Cluster analysis (Q-mode) showing the grouping of the identified palynofacies types (PT), in Mallín Quemado Norte section. Cophenetic correlation coefficient: 0.7768.

relief organic spheres (HROS, 1.4–3.4%; Fig. 5.8–9). The phytoclast group is present in a moderate proportion (27% on average) and is dominated by translucent particles (TP), mainly DBBK (2.4–18.6%) and DET (up to 16.6%). Blade-shaped "DBBK+DET+OP" prevail (68.6% on average) over the equidimensional ones (31.4% on average), except in UNS-PMQN5577 sample, where both types of particles are found in equal proportions and have similar dimensions (Fig. 7). Palynomorphs are scarce (2% on average) and are represented by spores, pollen grains and indeterminate forms (Fig. 5.1).

Most of the samples are non-fluorescent except for isolated particles that fluoresce heterogeneously or homogeneously to greenish-yellow and reddish-orange with weak, occasionally moderate intensity (e.g., granular AOM with transparent matrix, gAOMtm, and tubes). Nevertheless, samples UNS-PMQN5577 and UNS-PMQN5581 show some particles that fluoresce heterogeneously to green and yellow with moderate and strong intensity (Fig. 6.1–4). The average TOC is 2.46%.



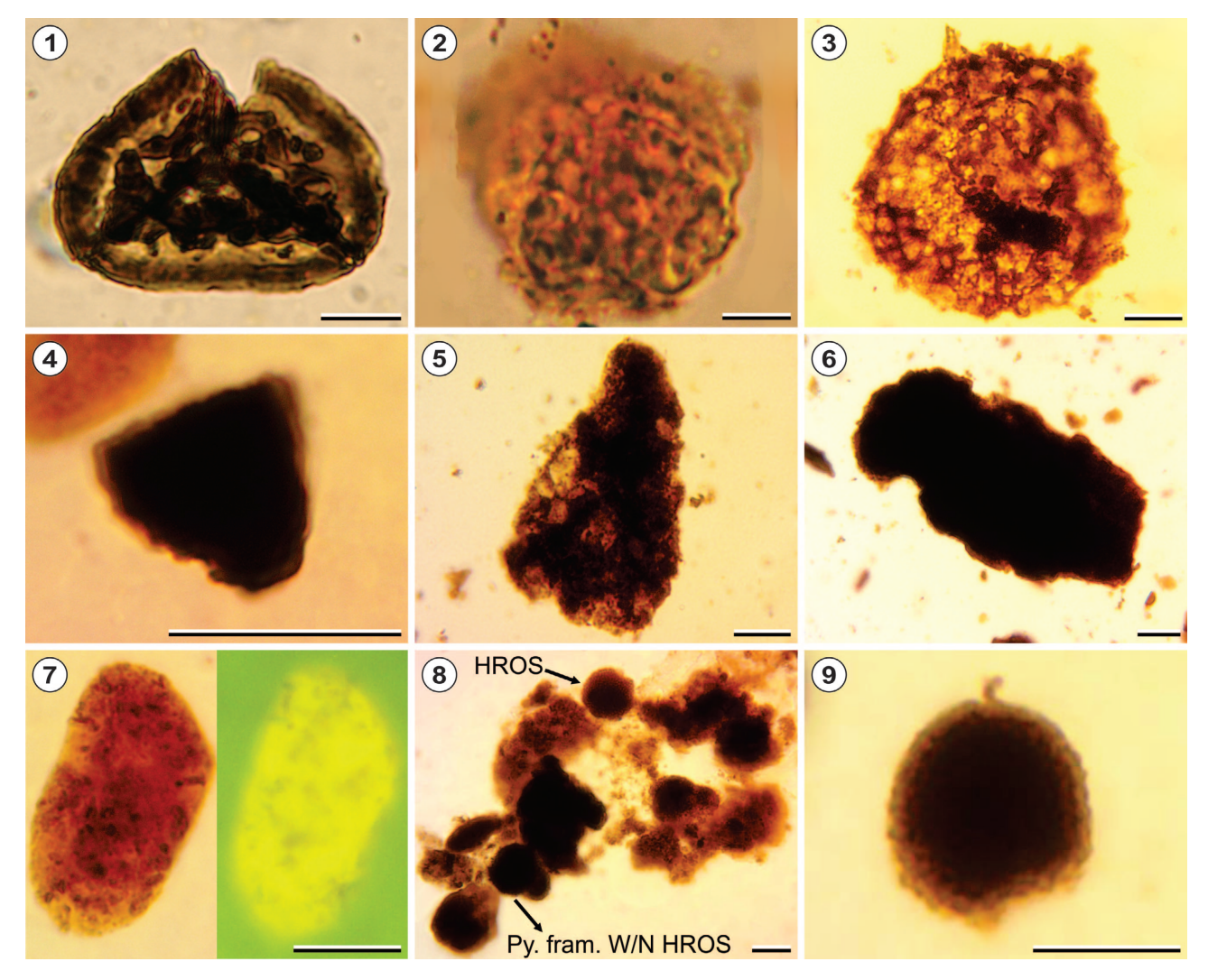


Figure 5. Selection of palynological matter that composes the kerogen of the studied levels of the Vaca Muerta Formation at Mallín Quemado Norte. 1, *Interulobites lajensis* Martínez, 2000, UNS-PMQN4634: R18/4. 2, Botryococcaceae algae, UNS-PMQN4853: B46/4. 3, Proximate dinocyst (probably *Cribroperidinium* sp.) with abundant crystal imprints, UNS-PMQN5580: W29/4. 4, Dark brown to black phytoclast, UNS-PMQN5585: S27/1. 5, Pelicular AOM, UNSPMQN5573: Q28/3. 6, bAOMte (see Tab. 1), UNS-PMQN5576: N29. 7, Pellet, UNS-PMQN5585: U27; under TWL showing granular amorphous organic matter appearance (left) and under RFL showing heterogeneous yellow fluorescence with moderate intensity (right). 8, HROS included in bAOMte, UNSPMQN5578: K20. See at the bottom left a pyrite framboid core within a high-relief organic sphere. 9, Detail of the HROS, UNSPMQN5576: S19. Scale bar= 10 μm. Abbreviations: HROS, high-relief organic spheres; RFL, reflected fluorescence light; TWL, transmitted white light.

PT B. In this PT, DBBK phytoclasts reach the highest proportions of all section (42.6–66.2%). Blade-shaped "DBBK+DET+OP" prevail (69.9% on average) over the equidimensional ones (30.1% on average). The AOM group is mainly composed of bAOMte (30% on average). Palynomorphs occur in very low quantities (0.4–7.2%) and are represented by indeterminate forms (0.4–1.6%). Sample UNS-PMQN5576 exhibits fungal spores (6%) and dinocysts (0.6%). Sample UNS-PMQN5585 contains the highest

proportion of pellets of all samples in the section (13.4%).

Most of the components of this PT are non-fluorescent, except for isolated particles that fluoresce heterogeneously to orange-yellow (*e.g.*, pellets), orange-red (Fig. 6.5–6) with moderate intensity and to greenish-yellow (Fig. 6.7–8) with weak intensity. It has also particles that fluoresce homogeneously with weak and moderate intensity to green and yellow respectively (Fig. 6.9–10). In sample UNS-PMQN5585 some components fluoresce heterogeneously

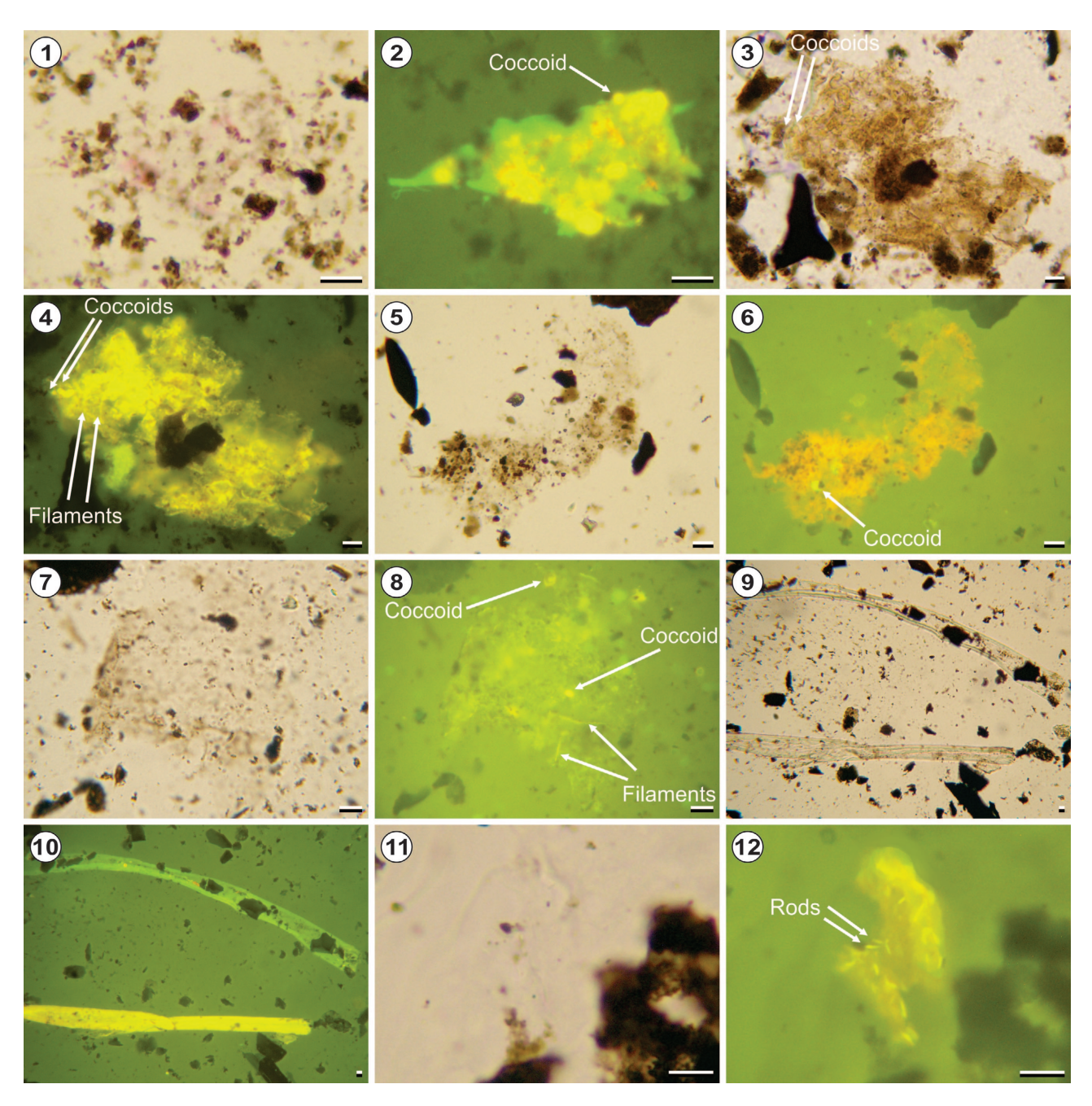
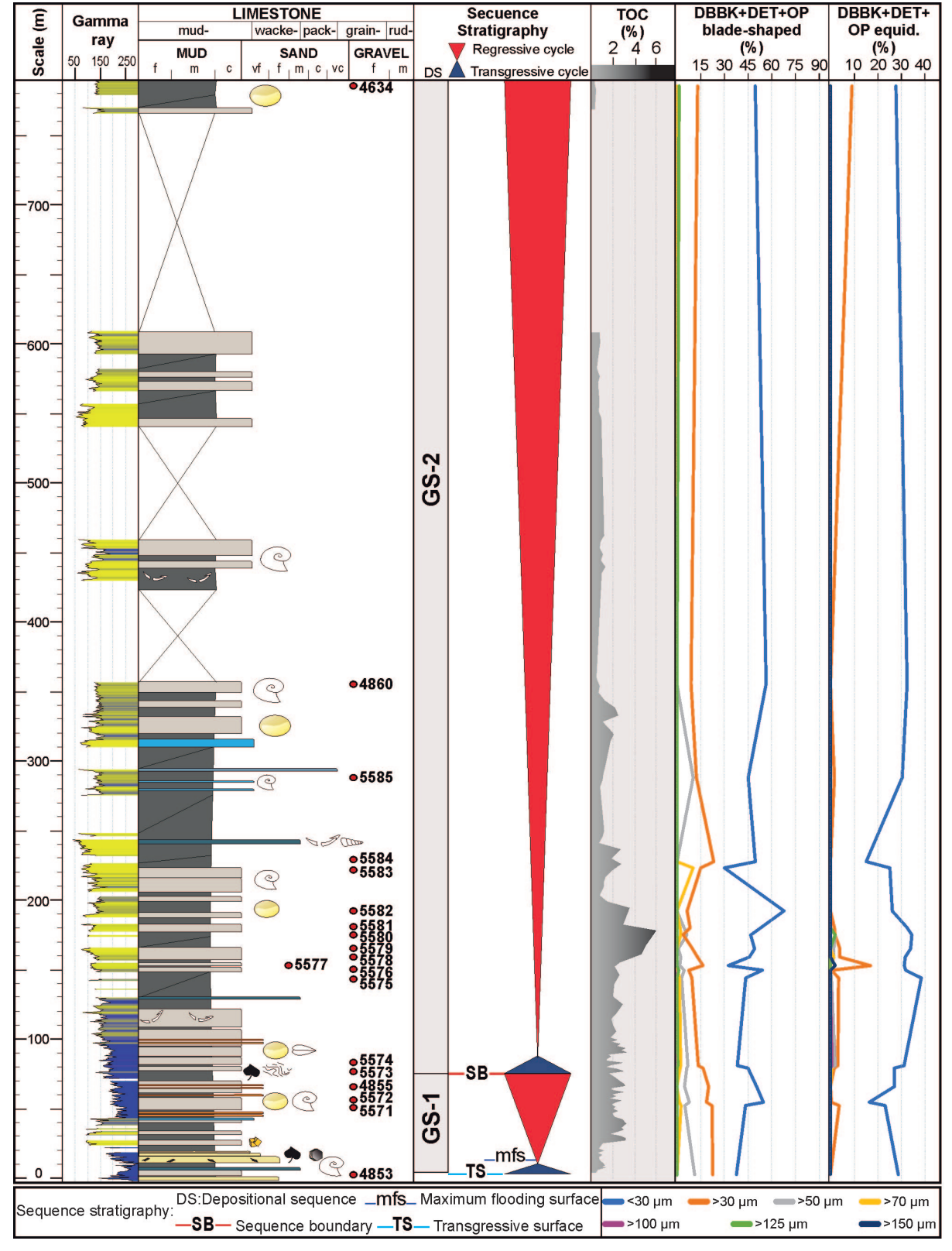


Figure 6. Selection of fluorescent palynological matter that composes the kerogen of the studied levels of the Vaca Muerta Formation at Mallín Quemado Norte. 1–2, gAOMtm (see Tab. 1), UNS-PMQN5577: K30/2; 1, under TWL scarcely visible by particle binding; 2, under RFL fluoresce heterogeneously, the matrix to green with moderate intensity and the coccoid bacteria to yellow with strong intensity. 3–4, gAOMtm, UNS-PMQN5581: Z15/4; 3, under TWL light brown mass binding particles and amber coccoid bacteria; 4, under RFL fluoresce heterogeneously, matrix to yellowish-green with moderate intensity, and coccoid bacteria and filaments to yellow with strong intensity. 5–6, gAOMtm, UNS-PMQN5573: F10; 5, under TWL scarcely visible by particle binding; 6, under RFL fluoresce heterogeneously, the matrix to orange-red with moderate intensity and the coccoid bacteria to yellow with moderate intensity. 7–8, gAOMtm, UNS-PMQN5571: J21/4; 7, under TWL scarcely visible by particle binding; 8, under RFL fluoresce heterogeneously, the matrix to greenish-yellow with weak intensity and coccoid bacteria and filaments to yellow with weak-moderate intensity. 9–10, Tubes, UNS-PMQN5573: W20; 9, under TWL more or less transparent tubes of large dimensions; 10, under RFL fluoresce homogeneously to green and yellow with weak and moderate intensity respectively. 11–12, Transparent AOM, UNS-PMQN5580: D20/2; 11, under TWL is unidentifiable; 12, under RFL fluoresce heterogeneously, the matrix to yellowish-orange with weak intensity and short rod-shaped bacteria to yellow with moderate intensity. Scale bar= 10μm. Abbreviations: RFL, reflected fluorescence light; TWL, transmitted white light.





**Figure 7.** Stratigraphic column studied at Mallín Quemado Norte with location of analyzed palynological samples, depositional sequences identified, total organic carbon curve (% TOC) and curves showing the dimensions of blade-shaped and equidimensional (equid.) **"DBBK+DET+OP"** (% with respect to the sum of the three types of particles per sample). Depositional sequences and % TOC from Otharán (2020). Abbreviations: **"DBBK+DET+OP"**, dark brown to black + deteriorated + opaque phytoclasts; **equid.**, equidimensional.

to orange with strong intensity and yellow with moderate intensity (e.g., pellets). The average TOC is 1.87%.

PT C. It is characterized by a high percentage of AOM (46.8, 53.4 and 64.2%) mainly represented by bAOMte (14.8–33%), with subordinated values of pelicular (5.8–17.8%) and granular (3.2–13.4%) types. Sample UNS-PMQN5578 has the highest amount of HROS (7%). The phytoclasts vary from ~27 to 45% (Fig. 3). Within this group, DET are dominant and reach the highest percentages of the entire section (19% on average). Blade-shaped "DBBK+DET+OP" prevail (60.9% on average) over the equidimensional ones (39.1% on average). Palynomorphs are found in relatively low percentages (1.6–11%) and are mainly represented by indeterminate forms (1.6–10.6%), except in the sample UNS-PMQN5579 where 0.4% of spores are recognized, and in the sample UNS-PMQN5580 where 1.2% of dinocysts are identified (with one

specimen probably belonging to Cribroperidinium sp.) (Fig. 5.3).

Under RFL microscopy, sample UNS-PMQN5579 shows isolated components that fluoresce heterogeneously to yellowish-green with weakly and moderately intensity (e.g., gAOMtm). The remaining two samples have some particles that fluoresce heterogeneously to yellow with weak-moderate and strong intensity (gAOMtm binding large particles, coccoid bacteria and filaments) and to yellowish-orange with moderate intensity (Fig. 6.11–12). The average TOC is the highest of all PT, 4.69%.

**PT D.** This PT has the highest proportion of granular AOM (32.5 and 42.7%). In UNS-PMQN4860, AOM dominates (55%) followed by phytoclasts (30%), while in UNS-PMQN4853, phytoclasts dominate (53.8%) followed by AOM (43.6%). Most of the phytoclasts are translucent (30 and 33.5%), of the DBBK type (17 and 22.5%). Blade-shaped

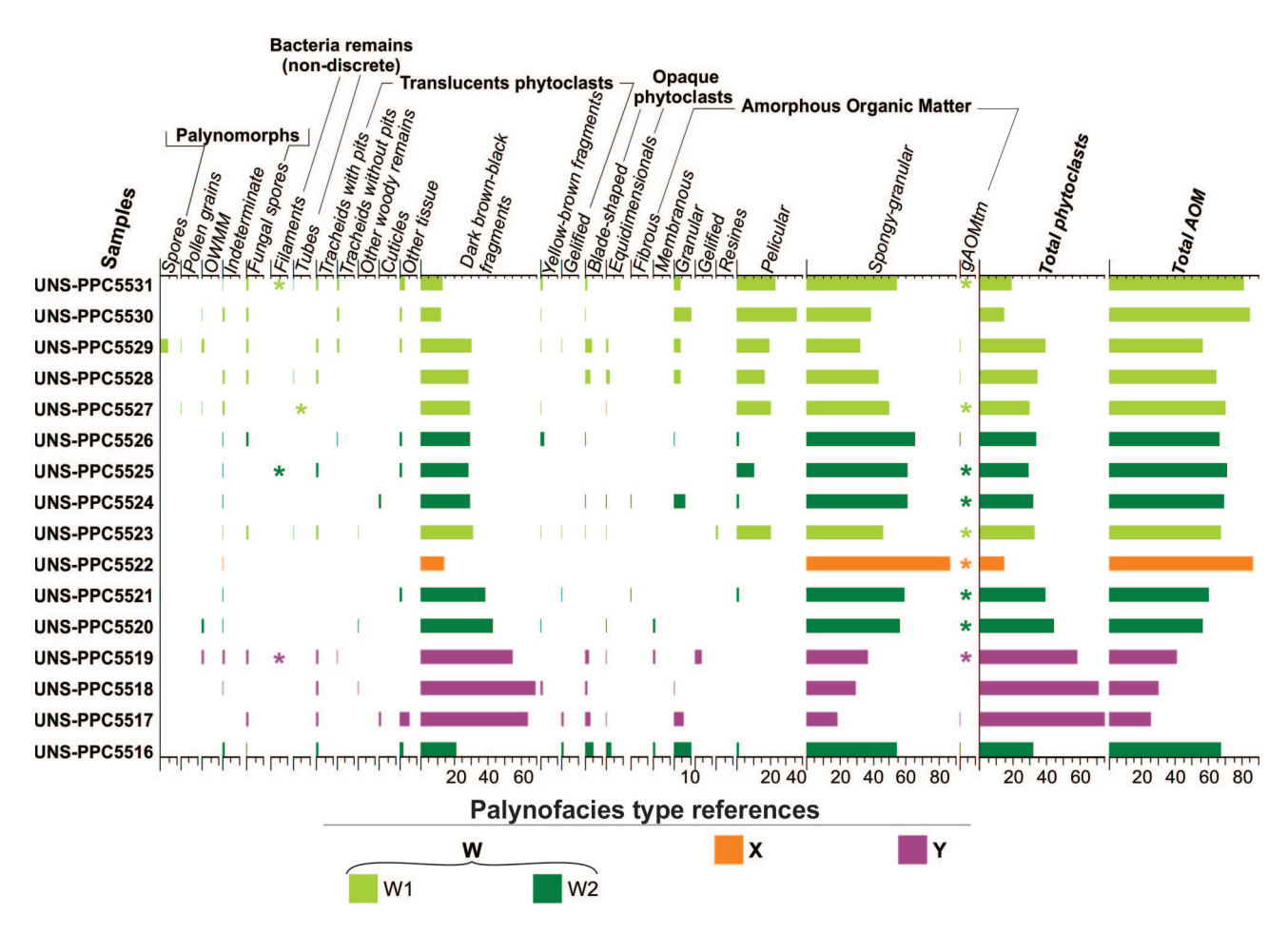


**Figure 8.** Relative frequency diagram (%) of the different palynological matter categories identified in the Puerta Curaco section. Based on the total count of 500 particles per sample. \* indicates presence.



"DBBK+DET+OP" prevail (69.2% on average) over the equidimensional ones (30.8% on average). Sample UNS-PMQN4853 has OP (20%), mostly blade-shaped (11.8%). Sample UNS-PMQN4860 has the highest percentage of palynomorphs in the section (15%), among which terrestrial forms predominate (79%), mainly represented by the families Hirmeriellaceae (45.9%) and Araucariaceae (20.8%). The rest of the palynomorphs (21%) correspond to OWMM (acritarchs and prasinophytes). In sample UNS-PMQN4853 algae of the family Botryococcaceae are present (Fig. 5.2).

The material is generally non-fluorescent, except for a few colorless or amber AOM masses that fluoresce faintly to pale yellow. The average TOC is 0.37%.

PT E. It is characterized by the high abundance of the phytoclast group (60-81.8%), mainly TP (56-37.2%), although it also shows the highest percentage of OP (23% on average). The TP are mainly represented by DBBK (17.2–24%) and DET (13% on average) fragments. Blade-shaped "DBBK+DET+OP" (57.8% on average) prevail (67.9% on average) over the equidimensional ones (32.1% on average). UNS-PMQN4855 has a relatively high percentage of AOM (40%), mainly of the spongy type (14%) and to a lesser extent of the fibrous type (11%). Sample UNS-PMQN4634 has palynomorphs (9%, mainly dark; Fig. 5.1), mostly terrestrial forms (93%). These terrestrial forms are pollen grains mainly from the families Hirmeriellaceae (42.8%), Podocarpaceae (15%), Araucariaceae (12.3%), Pinaceae (0.9%), and Caytoniaceae (0.9%). Trilete spores are also significant components of the assemblage (10.6%) and are mainly represented by the fern families Cyatheaceae/Dicksoniaceae/Dipteridaceae/Matoniaceae (2.6%), Hymenophylleaceae (1,8%) and Osmundaceae (1.7%). The remaining palynomorphs (7%) correspond to OWMM (dinocysts and sphaeromorphitae acritarchs).

None of the components exhibit fluorescence, except for a few colorless or amber AOM masses that fluoresce faintly to pale yellow. The average TOC is 0.95%.

# **Puerta Curaco section**

Based on the relative variations of 25 PM types in the PC section, three PT named W, X and Y and were identified from cluster analysis (Figs. 2, 8–9). Most palynomorphs within all PT are poorly preserved and mainly dark. Selected PM is illustrated on Figures 10.1–9 and 11.1–12.

PT W. This PT is the only palynofacies which has pelicular AOM (12.6% on average) and with the highest percentage of granular AOM (10.6%). The most abundant PM group is AOM (67.7% on average), followed by phytoclasts (31.1% on average). Within the AOM group, spongy-granular predominates (32.6–65%) and gAOMtm is consistently present in most samples, reaching the maximum values of the section (0.2–0.4%). Phytoclasts are mainly represented by DBBK (11.8–42.8%). Blade-shaped "DBBK+OP" prevail (84.8% on average) over the equidimensional ones (15.2% on average) (Fig. 12). It has the highest occurrence of non-discrete bacterial particles (up to 0,4%) (Fig. 8).

Two subpalynofacies (W1 and W2) emerged from the cluster analysis (Fig. 9). In W1, the pelicular AOM reaches the highest values (17.2–36.4%). Palynomorphs are scarce (0.2–1.4%) except in the sample UNS-PPC5529, where they reach their highest percentage (5.8%). Trilete spores dominate this group (4.4%) represented by scarcely ornamented spores and spores belonging to the Schizaeaceae and

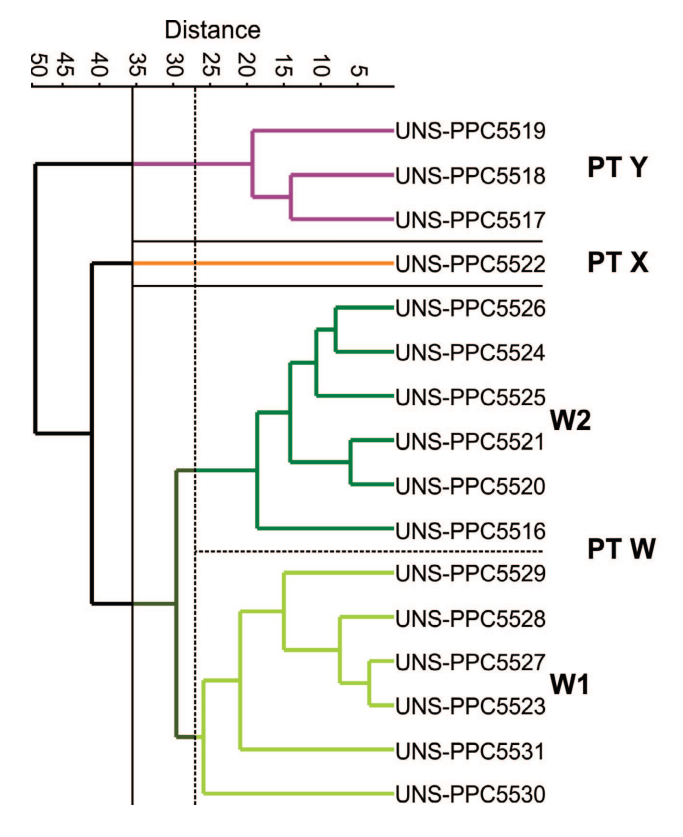


**Figure 9.** Cluster analysis (Q-mode) showing the grouping of the identified palynofacies types (PT) in Puerta Curaco section. Cophenetic correlation coefficient: 0.8095.

Osmundaceae families. Besides, bisaccate pollen grains (1%) and dinocyst (1%) are recognized. The dinocyst assemblage includes members of the Ceratiaceae family (Fig. 10.3). TOC values exhibit high variability, ranging from 3.8 to 10.3% (6.3% on average). W2 has the highest values of spongygranular AOM of the entire PT (except for PT X), relatively low percentage of pelicular AOM (2.4% on average) and is almost devoid of palynomorphs (0.5% on average). Sample UNS-PPC5516 has the highest percentage of granular AOM in the entire section (10.6%). TOC values vary from 1.9 to 9% (6.4% on average).

In W1, samples UNS-PPC5527–29 have some particles that fluoresce homogeneously to yellow (*e.g.*, cuticles) and green (*e.g.*, tubes, Fig. 11.1–2) with weak-moderate intensity, and scarce particles that fluoresce heterogeneously to greenish-yellow and yellow, with weak-moderate and strong intensity respectively (*e.g.*, gAOMtm, Fig. 11.3–4; gAOMtm with coccoid bacteria, Fig. 11.5–8). In W2, samples UNS-PPC5516/21/25 have isolated particles that fluoresce heterogeneously to yellowish-green, light yellow and reddish-orange with weak and moderate intensity (*e.g.*, gAOMtm with filaments, Fig. 11.9–10).

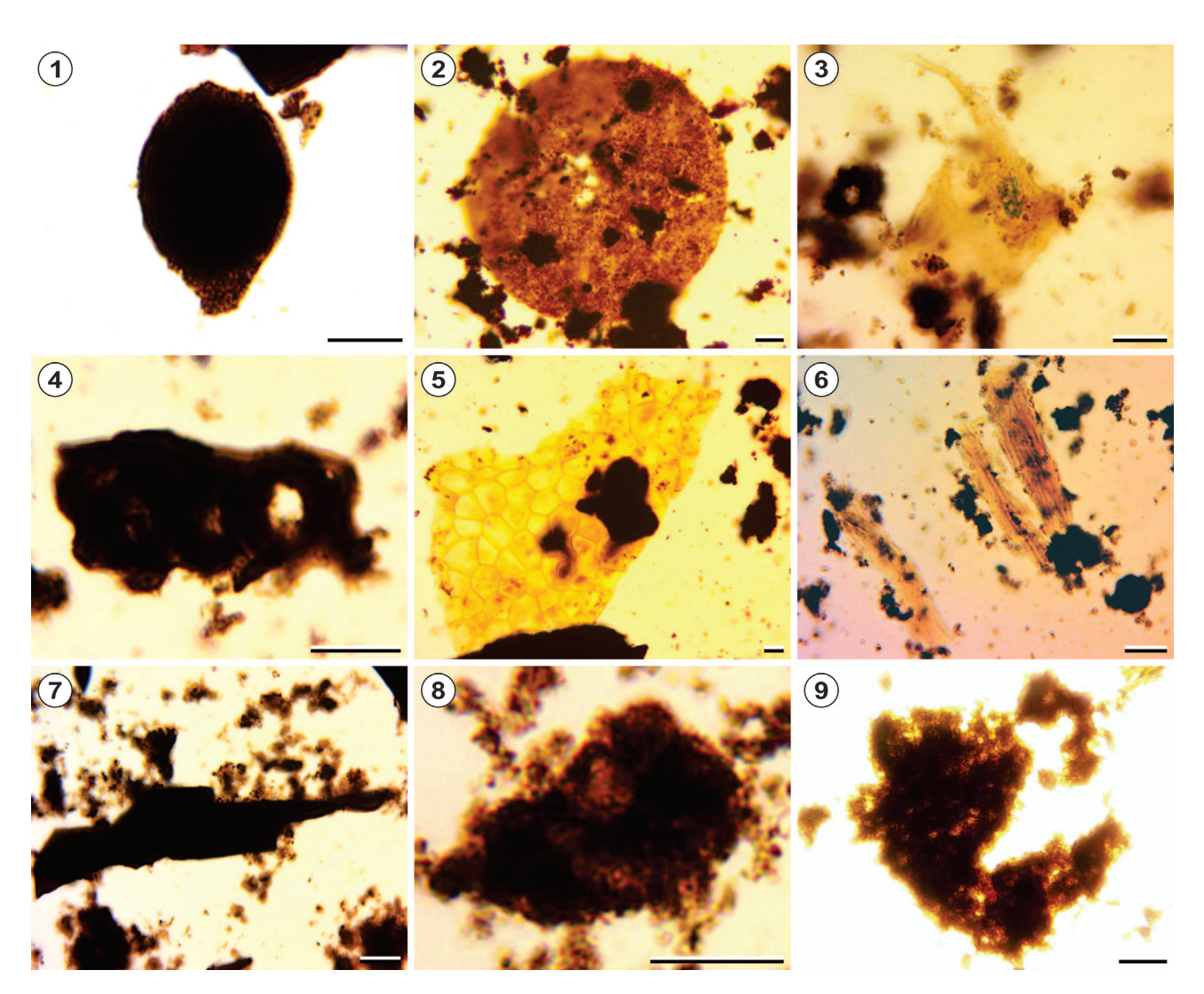


Figure 10. Selection of palynological matter that compose the kerogen of the studied levels of the Vaca Muerta Formation at Puerta Curaco. 1, 1-celled fungal spore, UNS-PPC5523: F24/4. 2, Prasinophyte indet., UNS-PPC5526: K6. 3, Dinocyst of the Ceratiaceae family, UNS-PPC5529: L13. 4, Partially deteriorated dark tracheid, UNS-PPC5529: F36/1. 5, Cuticle, UNS-PPC5528: P35. 6, Yellow to brown phytoclast, UNS-PPC5518: B14/3. 7, Dark brown to black phytoclast, UNS-PPC5523: Z28. 8, Spongy-granular AOM, UNS-PPC5520: S28/2. 9, Pelicular AOM, UNS-PPC5527: Y34. Scale bar= 10 μm.



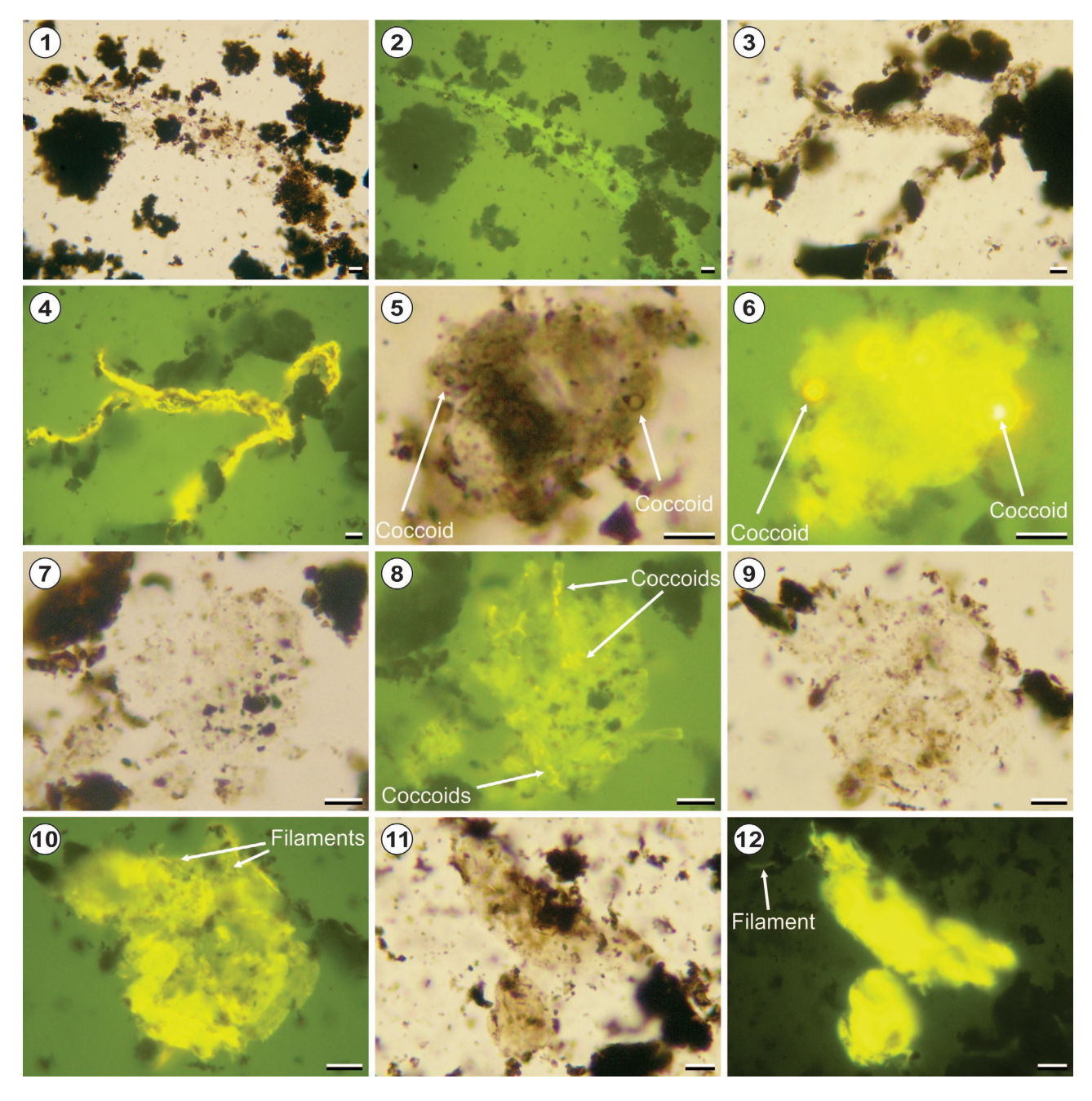


Figure 11. Selection of fluorescent palynological matter that composes the kerogen of the studied levels of the Vaca Muerta Formation at Puerta Curaco. 1–2, Tube, UNS-PPC5527: S7/1; 1, under TWL more or less transparent tube of large dimensions that binds particles; 2, under RFL fluoresce homogeneously to green with weak-moderate intensity. 3–4, gAOMtm (see Tab. 1), UNS-PPC5528: C36/3; 3, under TWL light brown elongate masses binding particles; 4, under RFL fluoresce heterogeneously to yellow with moderate and strong intensity. 5–6, gAOMtm, UNS-PPC5528: Q18/2; 5, under TWL brown mass binding particles and brown coccoid bacteria; 6, under RFL fluoresce heterogeneously, matrix to greenish-yellow with moderate intensity, and coccoid bacteria to yellow and orange with strong intensity. 7–8, gAOMtm, UNS-PPC5529: B10; 7, under TWL only partially identifiable by particle binding; 8, under RFL fluoresce heterogeneously, the matrix to greenish-yellow with weak-moderate intensity and coccoid to yellow with moderate intensity. 9–10, gAOMtm, UNS-PPC5525: E18; 9, under TWL only partially identifiable by particle binding; 10, under RFL fluoresce heterogeneously, the matrix to yellowish-green with weak and moderate intensity and filaments to yellowish-green with moderate intensity. 11–12, gAOMtm, UNS-PPC5519: L12/4; 11, under TWL light brown mass binding particles; 12, under RFL fluoresce heterogeneously, the matrix to yellow with moderate-strong intensity and filaments to yellowish-green with weak-moderate intensity. Scale bar= 10 μm. Abbreviations: RFL, reflected fluorescence light; TWL, transmitted white light.

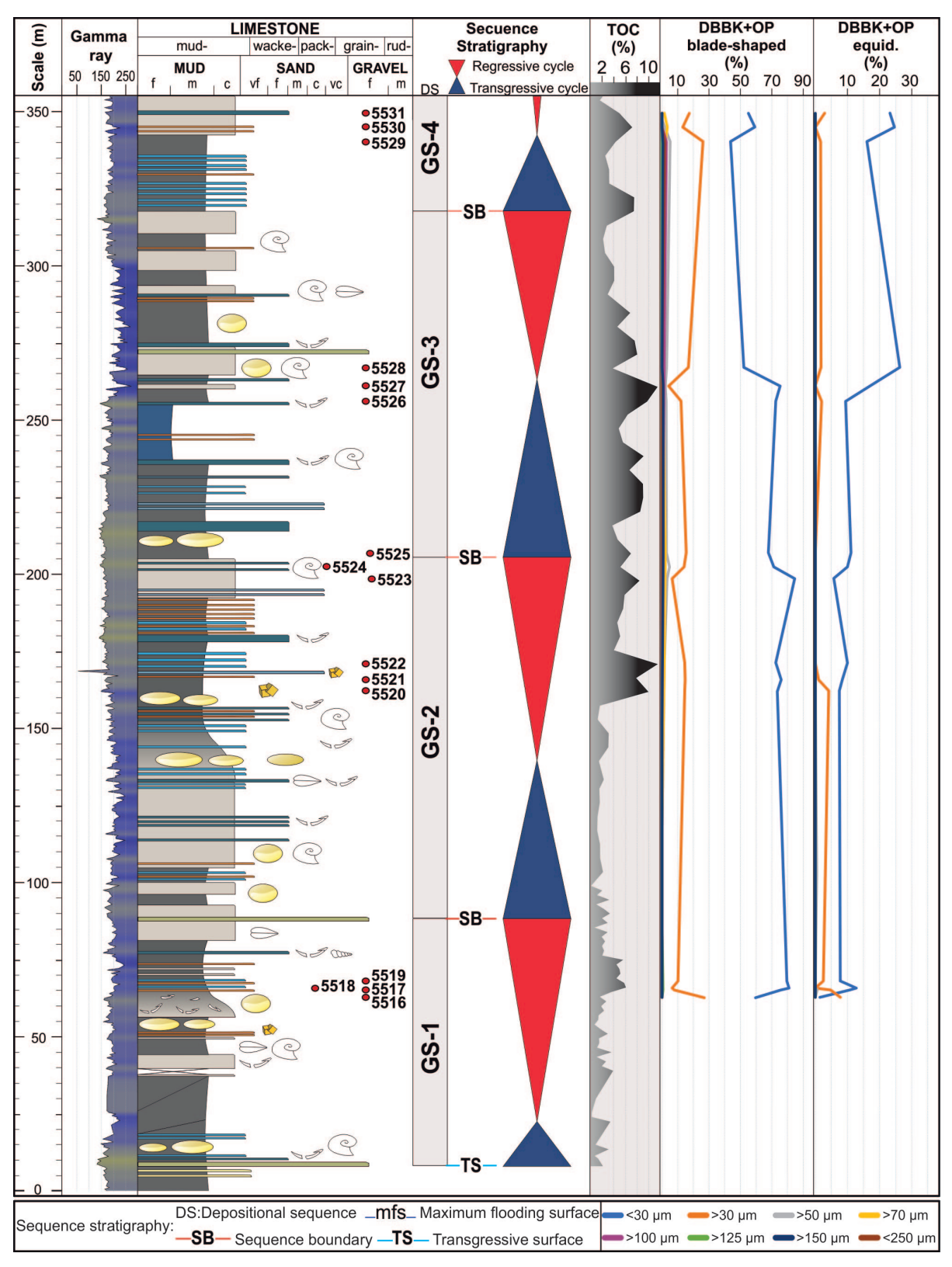


Figure 12. Stratigraphic column studied at Puerta Curaco with location of analyzed palynological samples, depositional sequences identified, total organic carbon curve (% TOC), and curves showing the dimensions of blade-shaped and equidimensional (equid.) "DBBK+OP" (% with respect to the sum of the two types of particles per sample). Depositional sequences and % TOC from Otharán (2020). Abbreviations: "DBBK+OP", dark brown to black + opaque phytoclasts; equid., equidimensional.



PT X. This PT is characterized by the highest percentage of spongy-granular AOM (86%, the only type of AOM). The phytoclast group consists only of DBBK (13.8%). Blade-shaped DBBK phytoclasts prevail (89.9%) over the equidimensional ones (10.1%). Palynomorphs are almost absent, only represented by indeterminate forms (0.2%).

None of the components fluoresce. TOC shows the highest value in all studied section (10.4%).

PTY. This PT is characterized by the highest values of DBBK phytoclasts (62% on average). It has the highest frequency of the phytoclast group in the entire section (57.8–74.4%). Blade-shaped "DBBK+OP" prevail (87% on average) over the equidimensional ones (13% on average); both particle types are represented in a fewer size's populations compared to the rest of the PT (Fig. 12). The AOM group is the second most abundant (24.6–41%) and is mostly represented by the spongy-granular type (18.4–37.2%). Palynomorphs are scarce (up to 1.2%) and are represented by OWMM (dinocysts), fungal spores, and indeterminate forms.

Under fluorescence, samples UNS-PPC5517 and UNS-PPC5519 show isolated particles that fluoresce heterogeneously to yellowish-green and yellow, with weak and slightly strong intensity respectively (gAOMtm with filaments, Fig. 11.11–12). The average TOC is 4.9%.

### DISCUSSION

# Mallín Quemado Norte section

Determining the origin of AOM from palynofacial analysis can be challenging. A useful tool is to evaluate the fluorescence of the material. The well-preserved AOM derived from algae and/or with a bacterial origin shows a much more intense fluorescence than that the one derived from aromatic (woody) structures, from terrestrial vascular plants (Bertrand *et al.*, 1986; Tyson, 1995; Batten, 1996a). However, the absence of fluorescence in bAOMte does not allow us to assume its origin, because this feature could indicate poor preservation of this material (Tyson, 1995).

Another alternative is to consider the rest of the palynological association, although this should be employed with caution (Batten, 1996a). bAOMte is widely represented throughout the section despite the variation in the nature of the palynological associations. However, it exhibits several partial correlations, including a mainly negative one

with granular AOM (microplankton or bacteria derived), suggesting incompatibility between their formation and/ or preservation conditions (Fig. 3). Additionally, it shows a partially positive correlation with phytoclasts, so it can't be entirely ruled out that part of this AOM could be derived from these constituents. Finally, it correlates positively with pelicular AOM almost throughout the section. Since pelicular AOM (sensu Combaz, 1980) has been associated with the degradation of microplankton or bacteria (Olivera et al., 2020) and/or secondary products of microbial activity on marine organic matter (Pacton et al., 2011), it's plausible that bAOMte is mainly of marine origin. However, it's not excluded that at least a minor portion of bAOMte is related to phytoclasts, which would reflect a mixed origin for this AOM.

A further option is to consider the type of sediment in which the AOM was preserved (Batten, 1996a). However, the variability and heterogeneity of fine-grained rocks are usually considerable, showing significant changes in terms of transport and depositional processes at centimeter-to millimeter scale. This is typical of the Vaca Muerta Formation (Otharán, 2020), consequently, the recurrent presence and in many cases the dominance of bAOMte throughout the entire section could be suggesting that its distribution is independent of the lithofacies.

The type and final characteristics of the AOM are controlled by its origin, depositional environment, thermal maturity and preservation state (Christiansen et al., 1989; Tyson, 1995; Batten, 1996a). AOM of different origins can be found in the same environment and can be composed of more or less deteriorated autochthonous and allochthonous particles (Pacton et al., 2011). bAOMte's variable features (shape, relief, edges) may suggest a different origin for these particles. This PM has essentially uniform color, possibly because they accumulated under similar depositional environment, where they would be subject to the same microbial activity and/or the same oxygen content (Pacton et al., 2011), or they experienced essentially a uniform degree of thermal maturity. Besides, the apparent bad preservation of this AOM (the absence of fluorescence) makes it challenging to determine its origin.

Microplankton or bacterial-derived AOM can be found originally disseminated in the rock matrix or concentrated

as discrete laminae (Tyson, 2006). Thus, it is valid to assume that the laminated bAOMte population (± elongated, with straight and angular edges), or at least part of it, would correspond to compacted and cohesive plastic organic laminae composed of fused AOM, which are broken during kerogen isolation (Tyson, 2006). Alternatively, it is not ruled out that part of this material corresponds to solid bitumen, which is a known and common component in some previous studies of the Vaca Muerta Formation (Małachowska et al., 2019; Petersen et al., 2020). In kerogen concentrates (acid-digested samples), when the original relationship between organic matter and the mineral matrix is destroyed, it becomes very difficult or even impossible to identify solid bitumen (Mastalerz et al., 2018). However, Fonseca et al. (2021), whose work primarily focuses on the characterization of solid bitumen using petrographic, palynological and geochemical techniques, note that solid bitumen particles in their palynological samples presented a smooth, fractured surface. This specific feature enabled them to distinguish solid bitumen from amorphous organic matter (Fonseca et al., 2021, fig. 3A-I). Since these characteristics were not identified in the present study, we assume that if solid bitumen is present, it is in such minor quantities that it does not affect the overall conclusions of our contribution.

Finally, bAOMte is morphologically very similar to AOMbr identified by Könitzer *et al.* (2016) in the Carboniferous mudstones. Following Könitzer *et al.* (2016) AOMbr would be of marine origin, although part of it could also be derived from plant-derived components (phytoclasts), and is independent of lithofacies. These conditions are similar to the ones proposed here for bAOMte.

The constant presence of pelicular AOM throughout most of the sequence would reflect the availability of carbonate during the deposition of the unit.

In all PT, "DBBK+DET+OP" <30  $\mu$ m represents 76.8% (on average) of the total of this fragment type, suggesting, in general terms, good sorting. For the same particle density, the particle size has more impact than shape on hydrodynamic behavior (Tyson, 1995), which could explain the high percentage of particles <30  $\mu$ m, in both bladeshaped and equidimensional fragments.

When the dimensions of the equidimensional and

blade-shaped fragments are analyzed separately, it is possible to identify a pattern present in all the PT (Fig. 7). The equidimensional phytoclasts are always represented in a fewer size's populations than those of blade-shaped phytoclasts, distributed in up to five or six populations. Thus, under the same flow hydrodynamic conditions, the equidimensional fragments respond better to transport sorting. Alternatively, this discrepancy could be attributed to differing transport and accumulation processes for each particle type. Blade-shaped fragments might have been transported from the continent via buoyant plumes, while equidimensional fragments could have been carried to the depositional site by traction currents. In this scenario, both components would be allochthonous, with the equidimensional particles exhibiting a longer residence time in the depositional environment compared to the blade-shaped.

**PT A.** The high percentage of bAOMte suggests that this PT is dominated by components of mainly marine origin.

Four samples in this PT have the same HROS identified by Emmings et al. (2019), according to personal communication of Emmings (2022). These spheres were originally recognized by Love (1957, 1962), who describes them as spherical forms covering the outer surface of pyrite framboids, and associates them with different types of microorganisms (e.g., Pyrithosphaera and microfossils of morphotypes 1-4). Emmings et al. (2019) identified the HROS surrounding pyrite framboids in marine deposits of the Bowland Shale Formation (Mississippian), UK. They relate their orange color to sulfurized organic matter (following Tribovillard et al., 2001). The authors associated HROS with high organic sulfur content and interpreted them as sulfurized organic matter local to pyrite framboids. Their formation is a product of redox oscillation between sulfidic and ferruginous anoxic microenvironments during early diagenesis (Emmings et al., 2019). Furthermore, Emmings et al. (2019) suggest that these spheres are mainly associated with an AOM that would correspond to zooplankton fecal minipellets and/or macro-zooplankter pellets (AOMpel) being this AOM abundant in mudstone deposited under anoxic and moderate to highly sulfidic conditions.

At MQN section, HROS were identified in the regressive hemicycle of GS-2 (Otharán, 2020), which is in agreement



with the observations of Emmings *et al.* (2019) who record them in levels deposited during sea level falls. In the Bowland Shale Formation, abundant HROS have been identified in deposits accumulated under anoxic bottom waters conditions, while scarce spheres have been recognized under sub-oxic bottom waters conditions (Emmings *et al.*, 2019). The levels of the Vaca Muerta Formation studied here are crypto-bioturbated and contain low percentages of HROS (up to 3.4%), suggesting that these sediments would not have accumulated under strictly anoxic bottom water conditions.

UNS-PMQN5574 shows the poorest sorting of "DBBK+DET+ OP", including both equidimensional and blade-shaped (Fig. 7). This could be due to the fact that this sample corresponds to mass transport deposits recognized at the top of the first depositional sequence (GS-1; Otharán, 2020).

According to palynological and sedimentological (Otharán, 2020) evidence, the deposition of the PT A would have occurred in an outer shelf environment during a period of quiescence characterized by relatively low and occasionally moderate (UNS-PMQN5574) terrigenous input to the basin. PM of marine origin (autochthonous) would have settled out from the water column (probably part as marine snow), while the terrestrial PM (allochthonous) would have been carried by plumes. After primary accumulation by fallout processes, organic carbon-rich mud would have been sporadically subject to resedimentation processes triggered by storm events, seismic activity and/or gravitational collapse of the subaqueous clinoform next to the shelf-break (UNS-PMQN5574).

PT B. The predominance of phytoclasts, with the exception of UNS-PMQN5585 sample, suggests a high terrigenous input. From base to top, the depositional environment of the Vaca Muerta Formation in MQN evolved from a shallow marine environment to a distally steepened mixed (siliciclastic-carbonate) shelf (Otharán, 2020). The presence of dinocysts, pellets, calcispheres, foraminifera and coccoliths recognized in this PT, reinforces the idea that it was deposited in an open marine environment relatively far away from detrital source areas.

UNS-PMQN5585 sample exhibits the highest percentage of both pellets (13.4%) and gAOMtm (2%) of the entire

section, and the best sorting of "DBBK+DET+OP" of this PT (Figs. 3, 7; Tab.1). Although direct relationships between the discovery of pellets in palynological preparations and productivity levels have not been conclusively established in the scientific literature, their presence likely indicates a non-negligible level of productivity.

Traditionally, it has been pointed out that the preservation of fecal pellets necessarily requires the presence of anoxic ocean bottom waters (Batten, 1996a), being the ideal conditions for their preservation anoxic bottom waters and sediments, or conditions of extremely high sedimentation rate and consequent low bioturbation (Robbins *et al.*, 1996 and references therein). Thus, if the conditions were not as previously mentioned, a substantial part of the pellets originated in the water column or in the benthos may rapidly degrade after deposition.

gAOMtm is composed of different agglutinated particles by a mainly transparent matrix. Consequently, in this study, this AOM is associated with extracellular polymeric substances (EPS) produced by microorganisms (e.g., bacteria, archaea and microeukaryotes) (e.g., Pacton et al., 2011; Decho & Gutierrez, 2017). In today's oceans, EPS corresponds to a wide variety of large molecules purposely produced as secretions of biofilms that secure attachment and enhance the local environment, and/or as metabolicexcess waste products (Decho & Gutierrez, 2017). In open marine waters, EPS can contribute to the formation of aggregates of organic and inorganic particles in the water column that, when heavy enough, sink to the bottom of the sea, known as marine snow (Alldredge, 2001). In addition, EPS is very abundant in microbial mats, where it contributes to the metabolic efficiency of the community (Neu, 1994) and favors the preservation of organic matter by trapping (Martínez et al., 2018b).

Recent contributions suggest that part of the pellets produced by planktonic organisms in the water column may form part of marine snow (Macquaker *et al.*, 2010; Otharán *et al.*, 2022), be encapsulated by EPS (Decho & Gutierrez, 2017; Martínez *et al.*, 2018a, 2018b) and thus get protected from degradation, abrasion and some grazer organisms during transport to and after being deposited on the ocean floor (Flemming *et al.*, 2016; Otharán *et al.*, 2022 and references therein).

UNS-PMQN5573 sample shows the poorest sorting of equidimensional "DBBK+DET+OP" and contains 1.2% of gAOMtm. The recovery of this sample from intrabasinal flow deposits related to slope instabilities could explain the presence of badly sorted of this kind of phytoclasts. Besides, due to this level is located immediately above a microbial bindstone (*i.e.*, microbial bioconstruction enriched in EPS that acts as a sediment trap, structured and amorphous organic matter), this type of granular AOM could be genetically related with this deposit.

In summary, the gAOMtm is associated with EPS and could have at least two origins along the entire section. In microbial mats developed in the bindstones levels immediately below sediment gravity flow deposits related to slope instabilities (PT A: UNS-PMQN5574, PT B: UNS-PMQN5573) and/or in open marine environments forming marine snow (rest of the samples) (Fig. 7). The transparent matrix of most gAOMtm masses (Tab. 1) suggests they may correspond to transparent exopolymer particles (TEPs in Decho & Gutierrez, 2017). This special kind of EPS is abundant in the upper part of the water column and plays an active role in the formation of marine snow (Wurl & Cunliffe, 2016).

The deposition of PT B would have occurred in an open marine environment, far from the source area, during pulses of high terrigenous input (e.g., UNS-PMQN5573, UNS-PMQN5575) alternating with periods of relative quiescence (UNS-PMQN5585). PM of continental origin would have been carried by plumes, while PM of marine origin would have been deposited by settling processes from the water column, probably as part of marine snow (e.g., dinocysts, pellets, calcispheres, bAOMte, gAOMtm). These settling processes from the water column would have been more representation during quiescence moments. The seafloor would have been a dynamic environment in which the previously deposited material could be reworked by tractive bottom currents.

**PT C.** The relatively high percentage of "bAOMte + pelicular AOM + granular AOM" (42.9% on average), the presence of dinocysts and pellets, and the moderate proportion of phytoclasts suggest that this PT would have accumulated in a shelf marine environment with moderate influence of terrigenous input (Tabs. 1–2). The degradation of phytoclasts

might occur by desiccation or oxidation, and/ or moldering by white rot fungi in the upper part of soils and peats (Tyson, 1995; Mendonça Filho *et al.*, 2012; Rodrigues *et al.*, 2021). Low values of the non-opaque, non-biostructured phytoclasts to deteriorated phytoclasts ratio have been associated with distal conditions (*e.g.*, Mendonça Filho *et al.*, 2011). Besides, DET particles could be the product of the abrasion and collision caused by advective sediment transport processes that were critical for the dispersion and accumulation of mud in offshore settings or could also be related to the reworking of older deposits by high-energy underflows with erosion capacity.

Spherical elements of the order of *ca.* 2.5–5.5 μm in diameter and filamentous elements of the order of *ca.* 1 μm in width included in gAOMtm (present in most PT) and short rod-shaped elements of *ca.* 4 μm in length included in transparent AOM would correspond to coccoid bacteria, bacterially derived filaments and short rod-shaped bacteria respectively (Fig. 6). This type of AOM was previously identified in the fossil record by Pacton (2007), Mendonça Filho *et al.* (2012) and Otharán *et al.* (2022), among others. The presence of EPS in the poorly preserved palynological association of MQN could be related to the extreme resistance to deterioration of this substance (Mendonça Filho *et al.*, 2012).

In UNS-PMQN5580 sample, the highest TOC of the entire section and the presence of pellets suggest moderate to high productivity in the water column.

Thus, the accumulation of PT C would have occurred in a shelfal depositional environment during a quiescence period characterized by pulses of relative increase in terrigenous input (UNS-PMQN5578 and UNS-PMQN5579 samples). The water column would have been enough nutrient-rich to support a moderate to high productivity. Part of the organic matter and fine-grained sediments would have been deposited by fallout processes. Terrigenous material could be transported into the basin via buoyant plumes or by density-driven muddy hyperpycnal flows that travelled for long distances until they reached distal depositional settings. The seafloor would have been reworked by advective sediment transport processes or by erosive currents.

PT D. The high proportion of granular AOM, the moderate



percentage of phytoclasts, and the presence of spores, Hirmeriellaceae, Araucariaceae, prasinophytes and acritarchs in UNS-PMQN4860 sample, suggest a shelfal depositional environment with moderate continental input (Tab. 2).

The co-occurrence of Hirmeriellaceae and Araucariaceae in this sample would suggest warm to temperate-warm and relatively humid climatic conditions (Vakhrameev, 1981; Quattrocchio et al., 2001). This community would have also developed in regions subject to periodic dry seasons (Abbink, 1998). The exine structure and morphology of the Araucariaceae pollen grains suggest that they are not transported by air currents over long distances (Caccavari, 2003); so, it is inferred that they are mainly transported by fluvial currents and are accumulated relatively near to terrestrial sources of sediments (e.g., Martínez et al., 1996; Olivera et al., 2015).

Although components recognized in the studied samples include abundant material originally delivered to the sediment-water interface by suspension settling processes (i.e., marine snow, hypopycnal plumes), there is substantial evidence of episodic sedimentation controlled by punctuated events of seafloor disturbance and erosion. In UNS-PMQN4853 level, palynological (20% of OP) and sedimentological evidence suggest that bottom-traction transport was a recurrent process and probably caused the reworking of the seafloor and the redistribution of organic carbon-rich mud across distal depositional settings. While, in UNS-PMQN4860 sample, the depositional scenario seems to be quite different. As a result of the progressive reduction in accommodation space in shallow-marine environments, muddy underflows were responsible for the basinward transfer of fine-grained sediments, resulting in the growth and progradation of subaqueous clinoforms.

PT E. The characteristics of the PM suggest close proximity to and/or redeposition from the fluvial-deltaic source(s), and/or an oxidizing environment in which other components have been selectively destroyed (Tab. 2). The PM identified in sample UNS-PMQN4634 is consistent with a shelf marine depositional environment (Tab. 2). The oxidizing environment would explain the high percentage of OP, DBBK and DET phytoclasts recognized in this PT, and possibly the low TOC.

Both samples were recovered in prograding depositional

cycles, although they are associated with different positions in the marine environment. The UNS-PMQN4855 sample associated with the GS-1 sequence and the UNS-PMQN4634 sample with the GS-2 sequence. Several authors have employed the OP to TP ratio (OP:TP) as a palynofacial parameter to determine proximal-distal trends (Tyson, 1995; Olivera et al., 2020; Chalabe et al., 2022). Sample UNS-PMQN4855 exhibits a higher OP:TP ratio (0.61) than sample UNS-PMQN4634 (0.44), suggesting the former would be associated with conditions more distal to terrigenous input. This aligns perfectly with Otharán's (2020) interpretations regarding the depositional environment of both levels, which proposes for sample UNS-PMQN4855, inner basin-slope (clinoform foreset facies) and for sample UNS-PMQN4634, shelf-offshore (clinoform bottomset facies). Additionally, the palynological spectrum of sample UNS-PMQN4634 is dominated by mainly waterborne palynomorphs "Hirmeriellaceae + Araucariaceae + spores", over anemophilous pollen, "Podocarpaceae + Pinaceae + Caytoniaceae", which is indicative of conditions rather close to the area of terrigenous input.

The dominant depositional process could correspond to some type of plume associated with dilute flows (UNS-PMQN4634), however, part of the material of this PT (UNS-PMQN4855) could also be related to some type of dense flow (muddy underflow) with erosive capacity that would transport the material (reworking) over long distances into the basin. This is consistent with the high percentage of "DBBK+DET+OP" present in this PT, probably representing reworked material from pre-existing deposits.

Hydrocarbon source potential. The average TOCs of 2.46% (PT A), 1.87% (PT B), 4.69% (PT C), 0.37% (PT D) and 0.95% (PT E) indicate fair-good, fair, very good, very poor, and poor-quality kerogens, respectively (*sensu* Cornford, 2005). AOM-rich PT tend to have higher TOC values.

The preservation of organic carbon in the organic-rich mudstones of the Vaca Muerta Formation in MQN may be, at least in part, related to the role of EPS as an encapsulator of organic matter. Encapsulation protects the organic components from mechanical/biogenic deterioration and creates localized anoxic conditions, even in the presence of an oxygenated water column. These conditions have already been reported for the deposits of the Vaca Muerta

Formation (Otharán *et al.*, 2022). Additionally, it is likely that the gAOMtm corresponds to TEP particles, which would facilitate the export of carbon from the top of the water column to the ocean floor (Wurl & Cunliffe, 2016).

The different components of the PT are associated with certain types of kerogens (e.g., Tyson, 1995; Martínez et al., 2008; Mendonça Filho et al., 2012). Emmings et al. (2019) identified the highest percentages of HROS associated with a mixture between type II-S and III kerogens. The main constituent of type II-S kerogen, rich in sulfur, is autochthonous marine materials. The PM recognized in this contribution suggests that the kerogen of the Vaca Muerta Formation in MQN exhibits components typical of type II and III; however, the practical absence of fluorescent particles aligns the kerogen with type III-IV, making it gas-prone or essentially inert as a hydrocarbon source. A pyrolysis Rock-Eval analysis would be suitable to confirm these interpretations. The scarce percentage of HROS (up to 7%) recognized in the Vaca Muerta Formation may be related to the kerogen type here recognized, and/or to that the conditions for their formation were non-optimal (see Emmings et al., 2019). This coincides with low sulfur content previously registered in the Vaca Muerta Formation in the central areas of the basin (Brisson et al., 2020).

Given the highly dark color of the PM, an over-mature state cannot be entirely ruled out.

The lack of fluorescence of almost all the samples, the low proportion of tissues (fragile and readily biodegradable) and the degradation or mechanical damage identified in most of the palynomorphs, all point to poor kerogen preservation (Tyson, 1995; Batten, 1996b). These data suggest that the Vaca Muerta Formation kerogen at MQN has negligible hydrocarbon potential.

#### Puerta Curaco section

In all PT, "DBBK+OP" <30  $\mu$ m represents 81.3% (on average) of the total of this fragment type, suggesting, in general terms, good sorting. The dominance of bladeshaped and equidimensional fragments <30  $\mu$ m likely reflects that at equivalent densities the particle size has a greater influence than shape on the hydrodynamic behavior.

When the dimensions of the equidimensional and blade-shaped fragments are analyzed separately, a pattern

is identifiable in all the PT, except in PT Y (Figs. 9, 12). Consistent with observations at MQN (see MQN section), the equidimensional phytoclasts are always represented in a fewer size's populations than those of blade-shaped phytoclasts, which are distributed in up to six or seven populations. Therefore, under the same flow hydrodynamic conditions, the equidimensional fragments would respond better to transport sorting. An alternative explanation for this discrepancy might be attributed to differing transport and accumulation processes for each particle type.

**PT W.** The dominance of spongy-granular AOM (microplankton derived), the presence of OWMM (*e.g.*, dinocysts and prasinophyte algae) and the relatively low-moderate proportion of phytoclasts suggest that this PT would have been deposited in a marine environment with a low-moderate terrigenous input (Tab. 2).

In W1, the co-occurrence of trilete spores and ceratioid dinocyts in outer ramp setting (Otharán, 2020) could be suggesting deposition from bottom currents that brings material from a shallow marine environment (Tab. 2). The increase of carbonate-rich strata from base to top of the section (GS2–GS4) (Otharán, 2020) coincides with the progressive increase of the pelicular AOM from base (W2) to top (W1) (Fig. 12). The highest TOC values may be related to the highest percentage of pelicular AOM (UNS-PPC5523/27/30).

The deposition of the PT W would have occurred in an outer ramp setting (shallowing from W2 to W1), predominantly during a quiescence period, with pulses of low and moderate terrigenous input to the basin. The increase in carbonate content towards the top of the section correlates with a decrease in terrigenous input (*i.e.*, phytoclasts) and is clearly evident in samples UNS-PPC5530-31 (Fig. 8). So, the high amount of autochthonous AOM could be the result of settling processes from the water column (probably marine snow promoted by the gAOMtm) rather than a continental supply. Part of the terrestrial PM would have been carried by bottom currents with erosion capacity from shallow marine environments (*e.g.*, "DBBK+OP"), and other portion probably by buoyant plumes.

**PT X.** The dominance of spongy-granular AOM and the highest AOM:phytoclast ratio suggest that PT X would have been deposited in a marine environment during a period



of minimal terrigenous input, perhaps associated with a considerable distance from the source area or an overall period of quiescence and starved sediment conditions (maximum flooding surface—mfs). The dominant depositional process is likely associated with settling from the water column (spongy-granular AOM). The high TOC of this sample is probably responding to conditions of minimal sediment supply (evidenced by a very low percentage of phytoclasts), which would have promoted a low dilution of organic matter.

PT Y. The dominance of phytoclasts and the presence of dinocysts could be indicating a high terrigenous input to the open marine environment, which is in agreement with a regressive hemicycle interpreted by sedimentological and stratigraphic proxies (GS1) (Figs. 8, 12; Tab. 2). Nevertheless, as the majority of the phytoclasts are dark, it is possibly to assume the reworking of oldest deposits by bottom currents. The latter may be the more plausible option considering the sedimentological standpoint (Otharán, 2020). The relatively better sorting of the bladeshaped and equidimensional "DBBK+OP" regarding the other PT, including the distribution of both particle types in 3 size populations, could be related to the fact that this PM underwent a longer transport, and was deposited in a more distal, basinal environment (shallowing from GS1-GS4).

Deposition of PT Y would have occurred in an open marine environment, where the seafloor would have been reworked by muddy underflows with the erosion capacity. These processes would have been in charge of the transport of terrestrial PM from a shallow-marine ramp to more distal basin environments.

Hydrocarbon source potential. The average TOCs of 6.3% (PT W1), 6.4% (PT W2), 4.9% (PT Y) and the TOC of 10.4% (PT X) suggest very good quality kerogens (*sensu* Cornford, 2005). AOM-rich PT tend to have higher TOC values. In addition, in several samples the spongy-granular AOM increase in conjunction with TOC.

As in MQN, the preservation of organic carbon in the organic-rich mudstones of the Vaca Muerta Formation may have been facilitated, at least in part, by the encapsulation of organic matter by EPS (gAOMtm) (Olivera *et al.*, 2023).

The recognized PM suggests that the kerogen exhibits

components typical of type II and III kerogens, with a predominance of type II. However, the practical absence of fluorescent particles places it in the type III-IV, making this material prone to gas or inert. Analysis of pyrolysis Rock-Eval would be suitable to confirm our appreciations.

The highly dark color of the PM suggests that an overmature state cannot be entirely ruled out.

The negligible fluorescence in most samples, low tissue proportions and the degradation or mechanical damage of most of the palynomorphs suggest poor kerogen preservation (Tyson, 1995; Batten, 1996b). Thus, the poor preservation state of the Vaca Muerta Formation kerogen at PC suggests a negligible hydrocarbon potential.

# **CONCLUSIONS**

The sorting of phytoclasts suggests that, in general terms, the PM from both sections is well-sorted. With the exception of the PT Y, under the same hydrodynamic flow conditions, equidimensional fragments respond better to transport sorting. Alternatively, this discrepancy may reflect differing transport and accumulation processes for each particle type.

This study provides the first mention and documentation of sulfurized organic matter local to pyrite framboids in the Vaca Muerta Formation. This finding suggests redox oscillation between sulfidic and ferruginous anoxic microenvironments during the early diagenesis. Additionally, the low percentages of HROS and the crypto-bioturbated strata suggest that these sediments would not have accumulated under strictly anoxic bottom water conditions.

In MQN, the Vaca Muerta Formation was likely deposited mainly in an outer shelf marine environment, with a variable continental input to the basin. From base to top, the samples studied in this contribution show a growing continental influence through the following PT: A, C–D, B and E. Such gradual change in the compositional pattern is related to a regional increase in the rate of sediment supply that caused a normal marine regression.

In PC, the Vaca Muerta Formation was mainly deposited in an outer ramp marine environment, with a variable terrigenous input, ranging from minimal to moderate.

The primary transport and accumulation processes proposed for the depositional sites studied herein involve

an interplay between settling from the water column (marine snow; autochthonous components) and buoyant plumes (allochthonous components), followed by the reworking of the seafloor by bottom currents and sediment gravity flows which would have played a key role in the dispersal and redistribution of mud throughout the basin. In MQN, sediment gravity flows were recurrent processes, likely related to the gravitational collapse of an inherited high-relief slope. Bottom currents and muddy underflows would have played a significant role in transferring material from shallower areas (continental and marine PM) to deeper areas of the basin.

Levels deposited by resedimentation processes related to storm events and slope instabilities (mass transport deposits) show the poorest sorting of "DBBK+DET+OP". In contrast, those accumulated primarily by settling show the best sorting.

The gAOMtm and transparent AOM, genetically related with EPS, could have at least two origins. In MQN, in microbial mats and/or in the open ocean water column forming part of the marine snow (probably part as TEP particles). This latter origin is also suggested for the gAOMtm in PC.

The palynomorph content identified in MQN suggests the accumulation of these deposits under a warm to temperate-warm, seasonal climate with the alternation of dry and humid periods.

In both sections, AOM-rich PT tend to have higher TOC values.

The preservation of organic carbon in the mudstones of the Vaca Muerta Formation in MQN and PC may be, at least in part, related to the role of EPS as an encapsulator of organic matter and, consequently, as an exporter of organic carbon. This mechanism could help to explain the exceptional preservation of organic carbon in shallowing upwards cycles recognized in the Vaca Muerta Formation, which resulted from the progradation and vertical stacking of multiple event mudstone beds.

Although some deposits in MQN and PC contain more than sufficient organic matter for hydrocarbon generation, the poor preservation state of the kerogen suggests a negligible hydrocarbon potential.

#### **ACKNOWLEDGMENTS**

The authors thank Dr. E. G. Ottone and Dr. M. L. Balarino for their helpful suggestions, which improved the final version of the manuscript. We are also grateful to the anonymous reviewers for their careful revision, insightful criticism, and valuable comments. Finally, we would like to thank Dr. J. F. Emmings for their personal communication, which provided crucial information regarding the HROS identification discussed in this work. This work was supported by the Consejo Nacional de Investigaciones Científicas y Técnicas (CONICET) [grant number PIP 514CO to M. A. Martínez] and the Secretaría General de Ciencia y Tecnología of Universidad Nacional del Sur (SEGCyT) [grant number PGI 24/H156 to M. A. Martínez].

#### REFERENCES

- Abbink, O. A. (1998). *Palynological investigations in the Jurassic of the North Sea region* [PhD Thesis, Universiteit Utrecht]. Retrieved from the Utrecht University repository on October 8, 2025.
- Agüero, L. S., Martínez, M. A., Olivera, D. E., & Villa, R. D. (2022). Nuevos aportes palinológicos de la Formación Vaca Muerta (Titoniano) en Puente del Arroyo Picún Leufú, Subcuenca de Picún Leufú, Cuenca Neuquina, Argentina. *Boletín de la Asociación Latinoamericana de Paleobotánica y Palinología*, 22, 40–41.
- Aguirre-Urreta, B., Naipauer, M., Lescano, M., López-Martínez, R., Pujana, I., Vennari, V., De Lena, L. F., Concheyro, A., & Ramos, V. A. (2019). The Tithonian chrono-biostratigraphy of the Neuquén Basin and related Andean areas: A review and update. *Journal of South American Earth Sciences*, 92, 350–367.
- Alldredge, A. (2001). Particle Aggregation Dynamics. In J. H. Steele (Ed.), *Encyclopedia of Ocean Sciences* (pp. 2090–2097). Academic Press.
- Anderberg, M. R. (1973). *Cluster analysis for applications*. Academic Press.
- Arregui, C., Carbone, O., & Leanza, H. A. (2011). Contexto tectosedimentario. *Geología y Recursos Naturales de La Provincia Del Neuquén, 18,* 29–36.
- Batten, D. J. (1996a). Palynofacies and palaeoenvironmental interpretation. In J. Jansonius & D. C. McGregor (Eds.), *Palynology: Principles and applications*, Vol. 3 (pp. 1011–1064). American Association of Stratigraphic Palynologists Foundation.
- Batten, D. J. (1996b). Palynofacies and petroleum potential. In J. Jansonius & D. C. McGregor (Eds.), *Palynology: Principles and applications*, Vol. 3 (pp. 1065–1084). American Association of Stratigraphic Palynologists Foundation.
- Bertrand, P., Pittion, J.-L., & Bernaud, C. (1986). Fluorescence of sedimentary organic matter in relation to its chemical composition. *Organic Geochemistry*, 10(1), 641–647.
- Brisson, I. E., Fasola, M. E., & Villar, H. J. (2020). Organic Geochemical Patterns of the Vaca Muerta Formation. In D. Minisini, M. Fantín, I. Lanusse Noguera, & H. A. Leanza (Eds.), *Integrated geology of unconventionals: The case of the Vaca Muerta play, Argentina* (pp. 297–328). American Association of Petroleum Geologists Memoir 121.
- Brocke, R. & Riegel, W. (1996). Phytoplankton responses to shoreline fluctuations in the Upper Muschelkalk (Middle Triassic) of Lower Saxony (Germany). *Neues Jahrbuch Fur Geologie Und Palaontologie - Abhandlungen, 200*, 53–73.
- Brugman, W. A., Van Bergen, P. F., & Kerp, J. H. F. (1994). A quantitative approach to Triassic palynology: The Lettenkeuper of the Germanic Basin as an example. In A. Traverse (Ed.), Sedimentation of organic particles (pp. 409–430). Cambridge University Press.



- Caccavari, M. (2003). Dispersión del polen en *Araucaria angustifolia* (Bert.) O. Kuntze. *Revista Del Museo Argentino de Ciencias Naturales Nueva Serie, 5*(2), 135–138.
- Chalabe, A. C., Martínez, M. A., Olivera, D. E., Canale, N., & Ponce, J. J. (2022). Palynological analysis of sandy hyperpycnal deposits of the Middle Jurassic, Lajas Formation, Neuquén Basin, Argentina. *Journal of South American Earth Sciences*, 116, 103867.
- Christiansen, F. G., Buchardt, B., Jensenius, J., Jepsen, H. F., Nøhr-Hansen, H., Thomsen, E., & Østfeldt, P. (1989). Bitumen occurrences. *Bulletin Grønlands Geologiske Undersøgelse*, 158, 61–72.
- Combaz, A. (1980). Les kérogènes vus au microscope. In B. Durand (Ed.), *Kerogen: Insoluble organic matter from sedimentary rocks* (pp. 55–111). Éditions Technip.
- Cornford, C. (2005). The Petroleum System. In R. C. Selley, L. R. M. Cocks & I. R. Plimer (Eds.), *Encyclopedia of Geology* (pp. 268–294). Elsevier.
- Decho, A. W. & Gutierrez, T. (2017). Microbial Extracellular Polymeric Substances (EPSs) in Ocean Systems. *Frontiers in Microbiology, 8,* Article 922.
- Domínguez, R. F., Leanza, H. A., Fantín, M., Marchal, D., & Cristallini,
   E. (2020). Basin Configuration during the Vaca Muerta Times. In
   D. Minisini, M. Fantín, I. Lanusse Noguera & H. A. Leanza (Eds.),
   Integrated geology of unconventionals: The case of the Vaca Muerta play, Argentina (pp. 141–161). American Association of Petroleum Geologists Memoir 121.
- Emmings, J. F., Hennissen, J. A. I., Stephenson, M. H., Poulton, S. W., Vane, C. H., Davies, S. J., Leng, M. J., Lamb, A., & Moss-Hayes, V. (2019). Controls on amorphous organic matter type and sulphurization in a Mississippian black shale. *Review of Palaeobotany and Palynology, 268*, 1–18.
- Flemming, H.-C., Neu, T. R., & Wingender, J. (2016). *The Perfect Slime: Microbial Extracellular Polymeric Substances (EPS).* IWA Publishing.
- Fonseca, C., Mendonça Filho, J. G., Lézin, C., Sobrinho da Silva, F., & Duarte, L. V. (2021). Solid Bitumen Occurrences in the Pyrenean Basin (Southern France): A Case Study across the Pliensbachian–Toarcian Boundary. *Minerals*, *11*, 1338.
- Garzon, S., Warny, S., & Bart, P. J. (2012). A palynological and sequence-stratigraphic study of Santonian–Maastrichtian strata from the Upper Magdalena Valley basin in central Colombia. *Palynology*, *36*, 112–133.
- González, G., Vallejo, M., Kietzmann, D., Marchal, D., Desjardins, P., Tomassini, F., Gomez Rivarola, L., & Dominguez, R. (Eds.). (2016). Transecta Regional de la Formación Vaca Muerta: Integración de sísmica, registros de pozos, coronas y afloramientos. Instituto Argentino del Petróleo y Gas.
- Grimm, E. C. (2004). *TGView* (Version 2.0.2) [Computer software]. Research and Collection Center, Illinois State Museum.
- Groeber, P. (1946). Observaciones geológicas a lo largo del meridiano 70°. 1. Hoja Chos Malal. *Revista de la Asociación Geológica Argentina, 1*(3), 177–208.
- Hammer, Ø., Harper, D. A., & Ryan, P. D. (2001). PAST: Paleontological statistics software package for education and data analysis. *Palaeontologia Electronica*, 4(1), 1–9.
- Howell, J. A., Schwarz, E., Spalletti, L. A., & Veiga, G. D. (2005). The Neuquén Basin: An overview. *Geological Society, London, Special Publications*, *252*(1), 1–14.
- Kietzmann, D. A., Llanos, M. P. I., & Iovino, F. (2022). Tithonian—Berriasian calcisphere (calcareous dinoflagellate cysts) zones in the Neuquén Basin, Argentina: Correlation between Southern Andes and Tethyan regions. *Newsletters on Stratigraphy, 56*(2), 157–185.

- Kietzmann, D. A., Palma, R. M., Riccardi, A. C., Martín-Chivelet, J., & López-Gómez, J. (2014). Sedimentology and sequence stratigraphy of a Tithonian–Valanginian carbonate ramp (Vaca Muerta Formation): A misunderstood exceptional source rock in the Southern Mendoza area of the Neuquén Basin, Argentina. Sedimentary Geology, 302, 64–86.
- Könitzer, S. F., Stephenson, M. H., Davies, S. J., Vane, C. H., & Leng, M. J. (2016). Significance of sedimentary organic matter input for shale gas generation potential of Mississippian Mudstones, Widmerpool Gulf, UK. Review of Palaeobotany and Palynology, 224, 146–168.
- Kovach, W. L. (1989). Comparisons of multivariate analytical techniques for use in pre-quaternary plant paleoecology. *Review of Palaeobotany and Palynology*, *60*(3), 255–282.
- Leanza, H. A. (1973). Estudio sobre los cambios faciales de los estratos limítrofes jurásico–cretácicos entre Loncopué y Picún Leufú, Provincia de Neuquén, República Argentina. Revista de La Asociación Geológica Argentina, 28, 97–132.
- Leanza, H. A. (2009). Las principales discordancias del Mesozoico de la Cuenca Neuquina según observaciones de superficie. *Revista Del Museo Argentino de Ciencias Naturales Nueva Serie, 11*(2), 145–184.
- Leanza, H. A., & Hugo, C. A. (1977). Sucesión de ammonites y edad de la Formación Vaca Muerta y sincrónicas entre los paralelos 35° y 40° l.s. Cuenca Neuquina-Mendocina. *Revista de La Asociación Geológica Argentina*, 32(4), 248–264.
- Leanza, H. A., Hugo, C. A., Repol, D., & Salvarredy Aranguren, M. (2003). Miembro Huncal (Berriasiano inferior): Un episodio turbidítico en la Formación Vaca Muerta, Cuenca Neuquina, Argentina. Revista de la Asociación Geológica Argentina, 58(2), 248–254.
- Legarreta, L. & Gulisano, C. A. (1989). Análisis estratigráfico secuencial de la Cuenca Neuquina (Triásico superior-Terciario inferior). Cuencas Sedimentarias Argentinas. Universidad de Tucumán, Serie Correlación Geológica, 6, 221–243.
- Legarreta, L. & Villar, H. J. (2011). Geological and geochemical keys of the potential shale resources, Argentina basins. *Search and Discovery*, Article 80196.
- Love, L. G. (1957). Micro-organisms and the presence of syngenetic pyrite. *Quarterly Journal of the Geological Society, 113*(1–4), 429–440
- Love, L. G. (1962). Further studies on micro-organisms and the presence of syngenetic pyrite. *Palaeontology*, *5*(3), 444–459.
- Macquaker, J. H. S., Keller, M. A., & Davies, S. J. (2010). Algal blooms and "Marine Snow": Mechanisms that enhance preservation of organic carbon in ancient fine-grained sediments. *Journal of Sedimentary Research, 80*(11), 934–942.
- Małachowska, A., Mastalerz, M., Hampton, L., Hupka, J., & Drobniak, A. (2019). Origin of bitumen fractions in the Jurassic-early Cretaceous Vaca Muerta Formation in Argentina: Insights from organic petrography and geochemical techniques. *International Journal of Coal Geology*, 205, 155–165.
- Martínez, M. A. & Quattrocchio, M. E. (2004). Palinoestratigrafía y palinofacies de la Formación Lotena, Jurásico Medio de la Cuenca Neuquina, Argentina. *Ameghiniana*, 41(3), 485–500.
- Martínez, M. A., Cuadrado, D. G., Bianchinotti, M. V., & Guerstein, G. R. (2018a). Palinomorfos no polínicos en matas microbianas modernas en un ambiente costero marginal (Bahía San Blas, Argentina). Libro de Resúmenes de la Reunión de Comunicaciones de la Asociación Paleontológica Argentina (p. 76). Puerto Madryn.
- Martínez, M. A., Cuadrado, D. G., Guerstein, G. R., & Bianchinotti, M. V. (2018b). Análisis palinofacial de sedimentos actuales

- colonizados por microorganismos en un ambiente costero marginal (Bahía San Blas, Argentina). *Libro de Resúmenes del XVII Simposio Argentino de Paleobotánica y Palinología* (pp. 144–145). Paraná.
- Martínez, M. A., García, V. M., & Quattrocchio, M. E. (1996). Análisis de componentes principales aplicado al estudio palinológico del Jurásico Medio de Cuenca Neuquina, Argentina. Actas del XIII Congreso Geológico Argentino y III Congreso de Exploración de Hidrocarburos (pp. 171–179). Buenos Aires.
- Martínez, M. A., Prámparo, M. B., Quattrocchio, M. E., & Zavala, C. A. (2008). Depositional environments and hydrocarbon potential of the Middle Jurassic Los Molles Formation, Neuquén Basin, Argentina: Palynofacies and organic geochemical data. *Andean Geology*, 35(2), 279–306.
- Mastalerz, M., Drobniak, A., & Stankiewicz, A. B. (2018). Origin, properties, and implications of solid bitumen in source-rock reservoirs: A review. *International Journal of Coal Geology, 195,* 14–36
- Méndez, V., Zanettini, J. C. M., & Zappettini, E. O. (1995). Geología y metalogénesis del orógeno Andino central, República Argentina. Secretaría de Minería, Anales 23, 1–190.
- Mendonça Filho, J. G., Menezes, T., & Mendonça, J. (2011). Organic composition (palynofacies analysis). *ICCP Training Course on Dispersed Organic Matter*, *5*, 33–81.
- Mendonça Filho, J. G., Menezes, T. R., de Oliveira Mendonça, J., de Oliveira, A. D., da Silva, T. F., Rondon, N. F., & da Silva, F. S. (2012). Organic facies: Palynofacies and organic geochemistry approaches. In D. Panagiotaras (Ed.), *Geochemistry–Earth's system processes* (pp. 211–248). Tech Rijeka.
- Minisini, D., Desjardins, P., Otharán, G., Paz, M., Kietzmann, D., Eberli, G., Zavala, C., Simo, T., Macquaker, J. H., & Heine, C. (2020b). Sedimentology, Depositional Model, and Implications for Reservoir Quality. In D. Minisini, M. Fantín, I. Lanusse Noguera & H. A. Leanza (Eds.), Integrated geology of unconventionals: The case of the Vaca Muerta play, Argentina (pp. 201–236). The American Association of Petroleum Geologists.
- Minisini, D., Fantín, M., Noguera, I. L., & Leanza, H. A. (Eds.). (2020a). Integrated Geology of Unconventionals: The Case of the Vaca Muerta Play, Argentina. The American Association of Petroleum Geologists.
- Naipauer, M., Comerio, M., Lescano, M. A., Vennari, V. V., Aguirre-Urreta, B., Pimentel, M. M., & Ramos, V. A. (2020). The Huncal Member of the Vaca Muerta Formation, Neuquén Basin of Argentina: Insight into biostratigraphy, structure, U-Pb detrital zircon ages and provenance. *Journal of South American Earth Sciences, 100*, 102567.
- Neu, T. R. (1994). Biofilms and microbial mats. In W. E. Krumbein, D. M. Paterson, & L. J. Stal (Eds.), *Biostabilization of sediments* (pp. 9–15). BIS-Verlag.
- Oboh-Ikuenobe, F. E. & de Villiers, S. E. (2003). Dispersed organic matter in samples from the western continental shelf of Southern Africa: Palynofacies assemblages and depositional environments of Late Cretaceous and younger sediments. *Palaeogeography, Palaeoclimatology, Palaeoecology, 201*(1), 67–88.
- Olivera, D. E., Martínez, M. A., Otharán, G., Agüero, L. S., & Zavala, C. (2023). First Tithonian record of perforated *Pediastrum* Meyen *s.l.* Species within early—diagenetic carbonate concretions from the Vaca Muerta Formation, Neuquén Basin, Argentina. Implications for the palynological analysis of fine-grained rocks. *Publicación Electrónica de La Asociación Paleontológica Argentina*, 23(2), 124–133.

- Olivera, D. E., Martínez, M. A., Zavala, C., Di Nardo, J. E., & Otharán, G. (2020). New contributions to the palaeoenvironmental framework of the Los Molles Formation (Early-to-Middle Jurassic), Neuquén Basin, based on palynological data. Facies, 66(23), 1–21.
- Olivera, D. E., Martínez, M. A., Zavala, C., Otharán, G., Marchal, D., & Köhler, G. (2018). The gymnosperm pollen *Shanbeipollenites* proxireticulatus Schrank from the Vaca Muerta Formation (Upper Jurassic–Lower Cretaceous), Neuquén Basin, Argentina. *Cretaceous Research*, *90*, 120–130.
- Olivera, D. E., Zavattieri, A. M., & Quattrocchio, M. E. (2015). The palynology of the Cañadón Asfalto Formation (Jurassic), Cerro Cóndor depocentre, Cañadón Asfalto Basin, Patagonia, Argentina: Palaeoecology and palaeoclimate based on ecogroup analysis. *Palynology*, *39*(3), 362–386.
- Otharán, G. (2020). Sedimentología y análisis de facies de la Formación Vaca Muerta (Tithoniano-Valanginiano) Cuenca Neuquina: El rol de los flujos de fango en la depositación de espesas sucesiones de lutitas [PhD Thesis, Universidad Nacional del Sur]. Retrieved from Universidad Nacional del Sur repository on October 8, 2025
- Otharán, G., Zavala, C., Arcuri, M., Di Meglio, M., Zorzano, A., Marchal, D., & Köhler, G. (2020). Análisis de facies en depósitos de grano fino asociados a flujos de fango. Formación Vaca Muerta (Tithoniano–Valanginiano), Cuenca Neuquina central, Argentina. *Andean Geology*, 47, 384–417.
- Otharán, G., Zavala, C., Arcuri, M., Marchal, D., Köhler, G., Di Meglio, M., & Zorzano, A. (2018). The role of fluid mud flows in the accumulation of organic-rich shales. The Upper Jurassic-Lower Cretaceous Vaca Muerta Formation, Neuquén Basin, Argentina. Actas del X Congreso de Exploración y Desarrollo de Hidrocarburos. Simposio de Recursos No Convencionales: Hacia Una Nueva Convención (pp. 61–90). Mendoza.
- Otharán, G., Zavala, C., Schieber, J., Olivera, D. E., Martínez, M., Díaz, P., Yawar, Z., & Agüero, L. S. (2022). Unravelling the fabrics preserved inside early diagenetic concretions: Insights for the distribution, accumulation and preservation of organic-rich mud in the interior of epicontinental basins. *Sedimentary Geology*, 440, Article 106254. https://doi.org/10.1016/j.sedgeo.2022. 106208
- Pacton, M. (2007). Geomicrobiological investigation of amorphous organic matter in fossil anoxic sediments and comparison with recent bacterial analogs [PhD Thesis, University of Geneva]. Retrieved from the Geneva University repository on October 8, 2025.
- Pacton, M., Gorin, G. E., & Vasconcelos, C. (2011). Amorphous organic matter—Experimental data on formation and the role of microbes. *Review of Palaeobotany and Palynology, 166*(3), 253–267.
- Paz, M., Buatois, L. A., Mángano, M. G., Desjardins, P. R., Notta, R., González Tomassini, F., Carmona, N. B., & Minisini, D. (2022). Organic-rich, fine-grained contourites in an epicontinental basin: The Upper Jurassic-Lower Cretaceous Vaca Muerta Formation, Argentina. *Marine and Petroleum Geology, 142*, Article 105757. https://doi.org/10.1016/j.marpetgeo.2022.105757
- Petersen, H. I., Sanei, H., Gelin, F., Loustaunau, E., & Despujols, V. (2020). Kerogen composition and maturity assessment of a solid bitumen-rich and vitrinite-lean shale: Insights from the Upper Jurassic Vaca Muerta shale, Argentina. *International Journal of Coal Geology*, 229, Article 103575. https://doi.org/10.1016/j.coal.2020.103575
- Prauss, M. L. (1989). Dinozysten-stratigraphie und palynofazies



- im Oberen Lias und Dogger von NW-Deutschland. Palaeontographica Abteilung B Paläophytologie, 214(1-4), 1-124.
- Prauss, M. L. (1996). The Lower Toarcian Posidonia Shale of Grimmen, Northeast Germany. Implications from the palynological analysis of a near-shore section. Neues Jahrbuch Für Geologie Und Paläontologie - Abhandlungen, 200(1-2), 107-132.
- Prauss, M. L. (2001). Sea-level changes and organic-walled phytoplankton response in a Late Albian epicontinental setting, Lower Saxony basin, NW Germany. Palaeogeography, Palaeoclimatology, Palaeoecology, 174(1), 221-249.
- Prauss, M. L. & Riegel, W. (1989). Evidence from phytoplankton associations for causes of black shale formation in epicontinental seas. Neues Jahrbuch Für Geologie Und Paläontologie, Monatshefte, 11, 671-682.
- Quattrocchio, M. E., García, V., Martínez, M., & Zavala, C. (2001). A hypothetic scenario for the Middle Jurassic in the southern part of the Neuquén Basin, Argentina. Publicación Electrónica de la Asociación Paleontológica Argentina, 7(1), 163-166
- Ramos, V. A., Naipauer, M., Leanza, H. A., & Sigismondi, M. E. (2019). The Vaca Muerta Formation of the Neuquén Basin: An Exceptional Setting along the Andean Continental Margin. In D. Minisini, M. Fantin, I. Lanusse, & H. A. Leanza (Eds.), Integrated geology of unconventionals: The case of the Vaca Muerta play (pp. 25-38). American Association of Petroleum Geologists
- Robbins, E. I., Cuomo, M. C., Haberyan, K. A., Mudie, P. J., Chen, Y. Y., & Head, E. (1996). Fecal pellets. In J. Jansonius & D. C. McGregor (Eds.), Palynology: Principles and applications, Vol. 3 (pp. 1085-1097). American Association of Stratigraphic Palynologists Foundation.
- Rodrigues, B., Silva, R. L., Mendonça Filho, J. G., Reolid, M., Sadki, D., Comas-Rengifo, M. J., Goy, A., & Duarte, L. V. (2021). The Phytoclast Group as a tracer of palaeoenvironmental changes in the early Toarcian. Geological Society, London, Special Publications, 514(1), 291-307.
- Salas, A. & Seiler, J. (1980). Termopalinología: Confiabilidad del método 'luz transmitida'. Primera parte. Boletín de La Asociación Latinoamericana de Paleobotánica y Palinología, 7, 23-37.
- Staplin, F. L. (1969). Sedimentary organic matter, organic metamorphism, and oil and gas occurrence. Bulletin of Canadian Petroleum Geology, 17(1), 47-66.
- Stinco, L. P. & Barredo, S. P. (2014). Vaca Muerta Formation: An example of shale heterogeneities controlling hydrocarbon accumulations. In S. I. Naruk & K. W. Fisher (Eds.), Unconventional Resources Technology Conference (URTec). American Association of Petroleum Geologists; Society of Exploration Geophysicists; Society of Petroleum Engineers.
- Stipanicic, P. N., Rodrigo, F., Baulies, O. L., & Martínez, C. G. (1968). Las formaciones presenonianas en el denominado Macizo Nordpatagónico y regiones adyacentes. Revista de La Asociación Geológica Argentina, 23(2), 67-98.
- Tahoun, S. S., Deaf, A. S., & led, I. M. (2018). The use of cyclic stratigraphic pattern of peridinioid and gonyaulacoid dinoflagellate

- cysts in differentiating potential thick monotonous carbonate reservoirs: A possible ecostratigraphic tool under test. Marine and Petroleum Geology, 96, 240-253.
- Traverse, A. (1994). Sedimentation of organic particles. Cambridge University Press.
- Traverse, A. (2007). Paleopalynology: Second Edition. Springer Netherlands.
- Tribovillard, N., Bialkowski, A., Tyson, R. V., Lallier-Vergès, E., & Deconinck, J. F. (2001). Organic facies variation in the late Kimmeridgian of the Boulonnais area (northernmost France). Marine and Petroleum Geology, 18(3), 371-389.
- Tyson, R. V. (1995). Sedimentary Organic Matter. Organic facies and palynofacies. Chapmal & Hall.
- Tyson, R. V. (2006). Calibration of hydrogen indices with microscopy: A review, reanalysis and new results using the fluorescence scale. Organic Geochemistry, 37(1), 45-63.
- Vakhrameev, V. A. (1981). Pollen Classopollis: Indicator of Jurassic and Cretaceous climates. Palaeobotanist, 28, 301-307.
- van de Schootbrugge, B., McArthur, J. M., Bailey, T. R., Rosenthal, Y., Wright, J. D., & Miller, K. G. (2005). Toarcian oceanic anoxic event: An assessment of global causes using belemnite C isotope records. Paleoceanography, 20(3). https://doi.org/10.1029/2004 PA001102
- Volkheimer, W., & Melendi, D. (1976). Palinomorfos como fósiles guía (3a parte). Técnicas de laboratorio palinológico. Revista Minera, Geología y Mineralogía. Sociedad Argentina de Minería y Geología, 34(1), 19-30.
- Weaver, C. E. (1931). Paleontology of the Jurassic and Cretaceous of West Central Argentina. University of Washington.
- Wurl, O., & Cunliffe, M. (2016). Transparent exopolymeric particles: An important EPS component in seawater. In H. C. Flemming, T. R. Neu, & J. Wingender (Eds.), The Perfect Slime: Microbial Extracellular Polymeric Substances (EPS) (pp. 249-267). IWA Publishing.
- Yrigoyen, M. R. (1991). Hydrocarbon resources of Argentina. 13° World Petroleum Congress, Special Issue, 38-54.
- Zavala, C., Lampe, J. M. M., Fernández, M., Meglio, M. D., & Arcuri, M. (2008). El diacronismo entre las Formaciones Tordillo y Quebrada del Sapo (Kimeridgiano) en el sector sur de la Cuenca Neuquina. Revista de la Asociación Geológica Argentina, 63(4), 754-765.

doi: 10.5710/PEAPA.09.09.2025.548

Recibido: 1 de julio de 2025 Aceptado: 9 de septiembre de 2025

Publicado: 3 de noviembre de 2025

Acceso Abierto Open Access

This work is

